doi: 10.3304/jmes.2020.16744 *Journal of Mediterranean Earth Sciences 12 (2020), 55-75*

J M E S **Journal of Mediterranean Earth Sciences**

Failure of the nourishment intervention at Ladispoli Beach (Central Latium coast, Italy), Part 2: the causes

Paolo Tortora *

Dipartimento di Scienze della Terra, SAPIENZA Università di Roma, Roma, Italy
** Corresponding author: 3333313796@tim.it*

ABSTRACT - This study focuses on the causes of the failure of a nourishment intervention that took place on a stretch of coast near Rome. Using data collected before and after this intervention, these causes have been researched through numerous inspections on selected aspects of possible relevance. The results obtained describe this nourishment as highly controlled by the grain size characteristics of the borrow sands, different from those of the local sediments. The equilibration of post-nourishment profiles occurred through erosion of a large part of the sand mass originally placed on the beach, and external redeposition of the eroded sand with formation of a large nearshore deposit. This dynamic was modulated by the availability of water space for deposition. Within the general progradational trend, distinct processes occurred along three belts parallel to the coast: in the inner belt, the steep pre-fill topography (positive shoreface accommodation) was mostly filled during nourishment operations; in the middle belt, the migration of the bar trough caused erosion on pre-existing morphology (negative accommodation); in the outer belt with high rates of sediment redeposition, the sediments in excess were expelled from the system (zero accommodation). Most of the methods used to explore this nourishment indicate that its failure is due to the borrow sand used, similar in size to the native sediment but considerably better sorted and, most importantly, with a relevant shortage of those sandy fractions instead present in the original beach. As a result, fill sands fed insufficiently the beach and excessively the breaking zone.

Keywords: Beach nourishment; Coastal modelling; Sedimentology; Ladispoli; Italian Tyrrhenian coast.

Submitted: 13 May 2020-Accepted: 20 June 2020

1. INTRODUCTION

The coast of the Province of Rome consists of several sandy beaches that traditionally attract a large number of people from the capital and surrounding cities in the summer, with relevant benefits to the local economies. The health of these beaches is closely linked to the sands delivered by the Tiber River, which are redistributed along a coast highly transformed by the urbanisation following the Second World War (Bellotti and De Luca, 1979; Caputo, 1989; AA.WW., 1995; Bersani and Bencivenga, 2001; Tarragoni et al., 2014; Bellotti et al., 2018). This coast underwent erosion in the last 60 years and many reparative interventions were performed, initially by hard structures and later, during the last 30 years, mostly by artificial nourishments (Caputo et al., 1987; Ferrante et al., 1993; Franco et al., 2004). A total of 17 main beach replenishments were completed, with the corresponding 5-6 million cubic meters of sand only partially stabilising the shoreline, which is still now in recession in several sectors (Regione Lazio, 2013).

One of these sectors is the Ladispoli Beach, located 35 km northwest of Rome (Fig. 1). This beach underwent erosion in its western extent mostly between 1955-1975, with over 100 m of shoreline recession in the most protruding coastal part (Mallandrino et al., 2014). After some attempts (between 1970-80) to counteract erosion through hard interventions, this beach was nourished in March 2003 but with negligible benefits. The beach widening was, in fact, on the order of 10 m a year after intervention, and the shoreline retreated further over the next few years to return to its original position.

The present study is an *a posteriori* exploration of this nourishment case aimed at clarifying the causes of its failure, also for the benefit of future nourishment actions. Thanks to a large set of monitoring data, these causes have been researched within the complex framework of interactions that nourishment disturbance typically generates (Bird and Lewis, 2015; De Schipper et al., 2016; Marinho et al., 2018; Huisman et al., 2019; Psuty et al.,

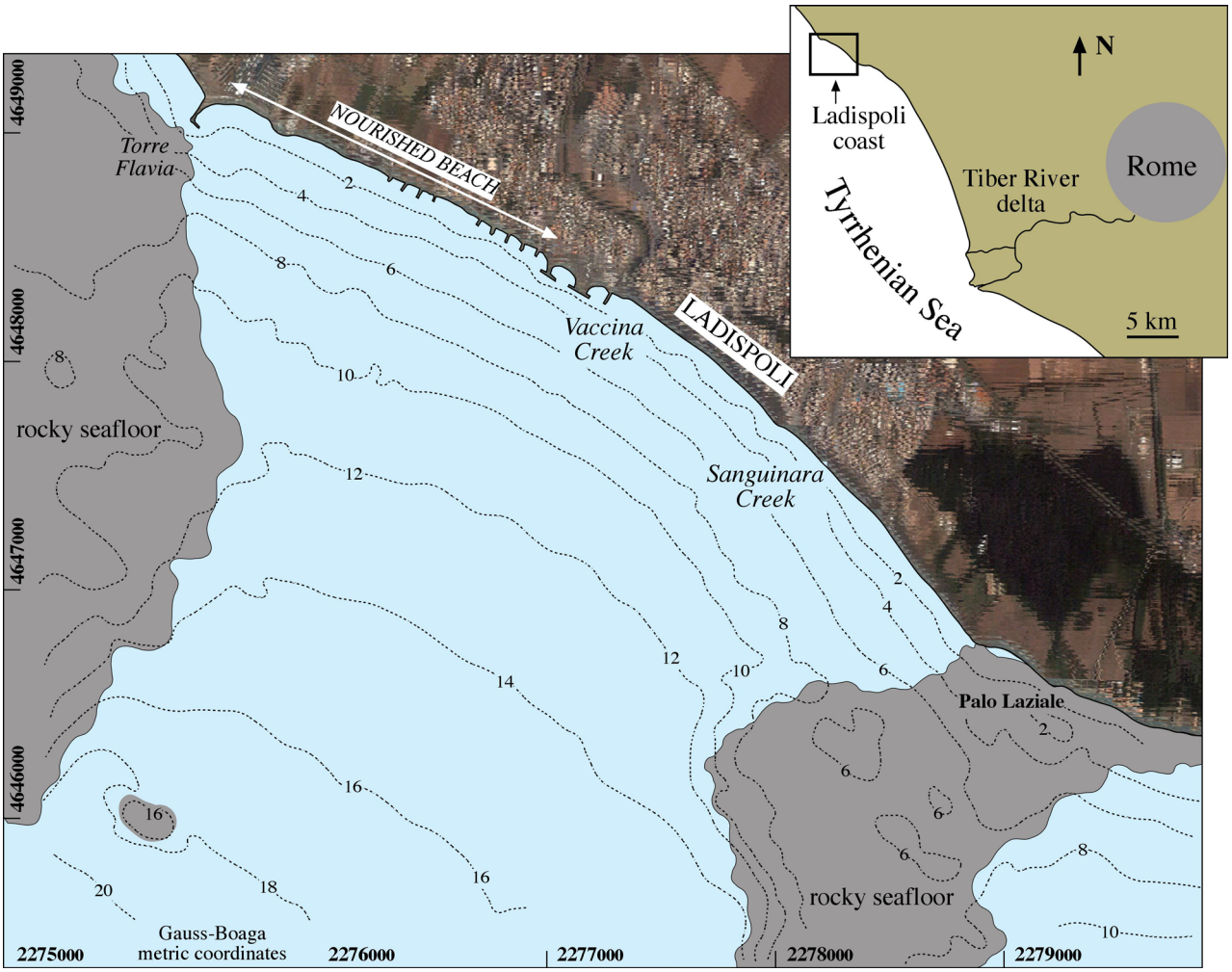

Fig. 1 - The physiographic coastal unit of Ladispoli with the beach nourished in March 2003.

2019). In this regard, numerous inspections were carried out on key aspects, also using virtual nourishment reproductions as a tool of exploration. Such key aspects have been selected considering the highlights in Tortora (2020, Part 1 in this volume), a paper that complements this study and includes some topics omitted here.

2. DATA AND METHODS

This study uses a portion of the original and processed data in Tortora (2020, part 1 in this volume: see Tab. 1). In particular, the main block of information is derived from three topo-bathymetric surveys carried out shortly before the intervention (03.2003), shortly after its completion (04.2003), and a year later (04.2004). Further data, concerning the grain size characteristics of superficial sediments (192 samples), were collected before nourishment (in 06.2001) and after (06.2005). All samples, including those of the quarry marine area, were analysed by a laser granulometer with a size resolution of 1/4 phi (Celia Magno et al., 2018). The statistical sediment parameters reported in some figures and in the main text refer to the method in Folk and Ward (1957). Most of the aforementioned data have been used to describe or forecast the artificial deposit, here considered as the nourishment derived deposit that is encapsulated between pre-fill (03.2003) and post-fill (04.2004) morphologic surfaces.

The cluster analysis on the cross-shore sections of this deposit (Section 3.2.) is based on the Euclidean distance with complete linkage method (Everitt et al., 2011). For each deposit section, the processed data consisted of thickness values regularly spaced in a cross-shore direction in reference to a common baseline (*i.e.* the pre-fill shoreline). In the data matrix used in the cluster process, the thicknesses along the baseline occupy a specific matrix row. Therefore, the pre-fill shoreline was considered as rectified to avoid the influence of coastal curvatures on the final results.

The estimates of the depth of closure by wave parameters (Section 3.3.) are based on data from the Rete Ondametrica Nazionale (ISPRA, http://dati.isprambiente.it/dataset/ron-rete-ondametrica-nazionale/), recorded from a buoy off the Civitavecchia coast (25 km from Ladispoli Beach) during the period of April 2003 - March 2014. A portion of these data was also used to reconstruct

the wave climate during the shorter period of April 2003 - March 2004 (Section 4.1.).

Information on the cores collected in the marine quarry area (Section 4.2.) is derived from laboratory data (Regione Lazio, 2003), updated through the exhumation of the original cores. This information concerns stratigraphic evidence, and results of grain-size analyses on samples representing core portions with apparently constant textural characteristics. The composite frequency distribution of the borrow material was calculated as the average (fraction by fraction) of all collected samples, weighing the fractions (%) by the length of the core portion that each sample represented.

The composite frequency curve related to the native sediments was estimated as the average (fraction by fraction) of single samples, using a procedure that obviates to their irregular geographic distribution (Section 4.2.). Specifically, each size fraction (%) was used in a spatial gridding process, then the sum of data in each grid was expressed as a percentage with respect to the sum of data in all grids. The composite native sample representing the sediments along individual cross-shore profiles was similarly calculated (sections 4.3.2. and 5.), as well as the average grain size distribution of the sediments eroded on pre-fill morphology (Section 4.5.). In the latter case the granulometric data, within isolated grid portions (with erosional features), were weighted based on the corresponding values of the erosional cuts.

The volumetric estimates (Section 4.5.) were based on grid thickness data whose layouts (isopach maps) are reported in Tortora (2020, part 1 in this volume: Fig. 8 A,C). These estimates omitted the westernmost area (120 m of coastline) with scattered rocky seafloor, as well as areas beyond the inner closure depth (*sensu* Hallermeier, 1981; Birkemeier, 1985), where sand veneer of possible nourishment derivation is here discontinuously present but with thicknesses (0-20 cm) often close to or below the instrumental resolution threshold.

Virtual nourishment reproductions (Section 5.) were performed by the Grain-size Nourishment Model (Tortora, 2008). This model uses topo-bathymetric and granulometric data (frequency distributions) that describe the pre-fill cross-shore profile to predict its evolution according to three variables: (1) the quality and (2) amount of the borrow material, and (3) the cross-shore boundaries of the pre-fill active beach profile. In the simulations shown, the first variable corresponds to the composite borrow sand frequency distribution (Fig. 5C), while the second and third variables were assigned according to data extracted from the local artificial deposit, specifically its volume and its cross-shore boundaries. The simulations by this model are the result of mathematical processes that distribute above the pre-fill profile the volume associated with each fraction of the borrow material. This process is regulated by the content (%) of the native fractions present before nourishment. Virtual sedimentation occurs fraction by fraction, and the sum of the formed "sediment layers" (one for fraction) reconstructs the artificial deposit. Details on theoretical aspects and model processes are reported in Guillen and Hoekstra (1996) and Tortora (2008), respectively.

3. PRELIMINARY

3.1. NOURISHMENT PROJECT

Following the requests of the local community, the technical office of the Regional Council (Regione Lazio) proceeded to plan an intervention at Ladispoli Beach aimed at both promoting recreational activities and preventing coastal damage during marine storms. Beach widening by artificial sand replenishment was the chosen solution in light of the existing chronic paucity of sediment. Alternative solutions by coastal defence structures were likely rejected to avoid further aesthetic detriment along the coast, down-drift erosional hot spots, and nearshore rip-circulation close to the eventual new structures. The project intended to widen the beach by about 35 m after profile equilibration. The needed sand volume was estimated at 270-300 m^3/m using conventional techniques based on the equilibrium beach profile method and granulometric comparisons between native and borrow sands (Regione Lazio, 2003). Four topo-bathymetric surveys were scheduled, to plan the intervention (first survey, February 2002), to count the sand volume used (second and third surveys, March and April 2003), and to ascertain the beach evolution a year after nourishment operations (fourth survey, April 2004). The intervention was performed in March-April 2003 by placing the fill sands on the dry beach and in very shallow water, harmonizing the berm at about a height of 2 m by levelling works.

3.2. GEOMETRY OF THE ARTIFICIAL-DEPOSIT

A year after nourishment, the artificial deposit appeared heavily reshaped by the waves showing rather variable characteristics along the coast. Its geometric variability is highlighted here by combining objective geological evidence with the results of a cluster analysis that was performed on thickness data of 35 cross-shore deposit sections. In the hierarchic cluster dendrogram, these sections can be joined into four main groups (Fig. 2A). Groups 1 and 2 (in light-blue and green colours) identify coastal zones A and B, respectively. Group 3, including few deposit-sections (in blue), is exclusive to zone C, whereas the Group 4 consists of ubiquitous sections (in red).

In light of objective geological evidence, the artificial deposit present in coastal zone A changes geometry quite gradually moving eastward from fairly uniform littoral prisms (Fig. 2B: section 1) to prisms that are increasingly fragmented into two sedimentary bodies by the bar trough (sections 5 and 10). This lateral transition is linked to the substrate morphology which controls the geometry of the overlying littoral prisms and, through its morphological highs (the rocky seafloor, Fig. 1), the degree of coastal exposure that increases in progression moving eastward.

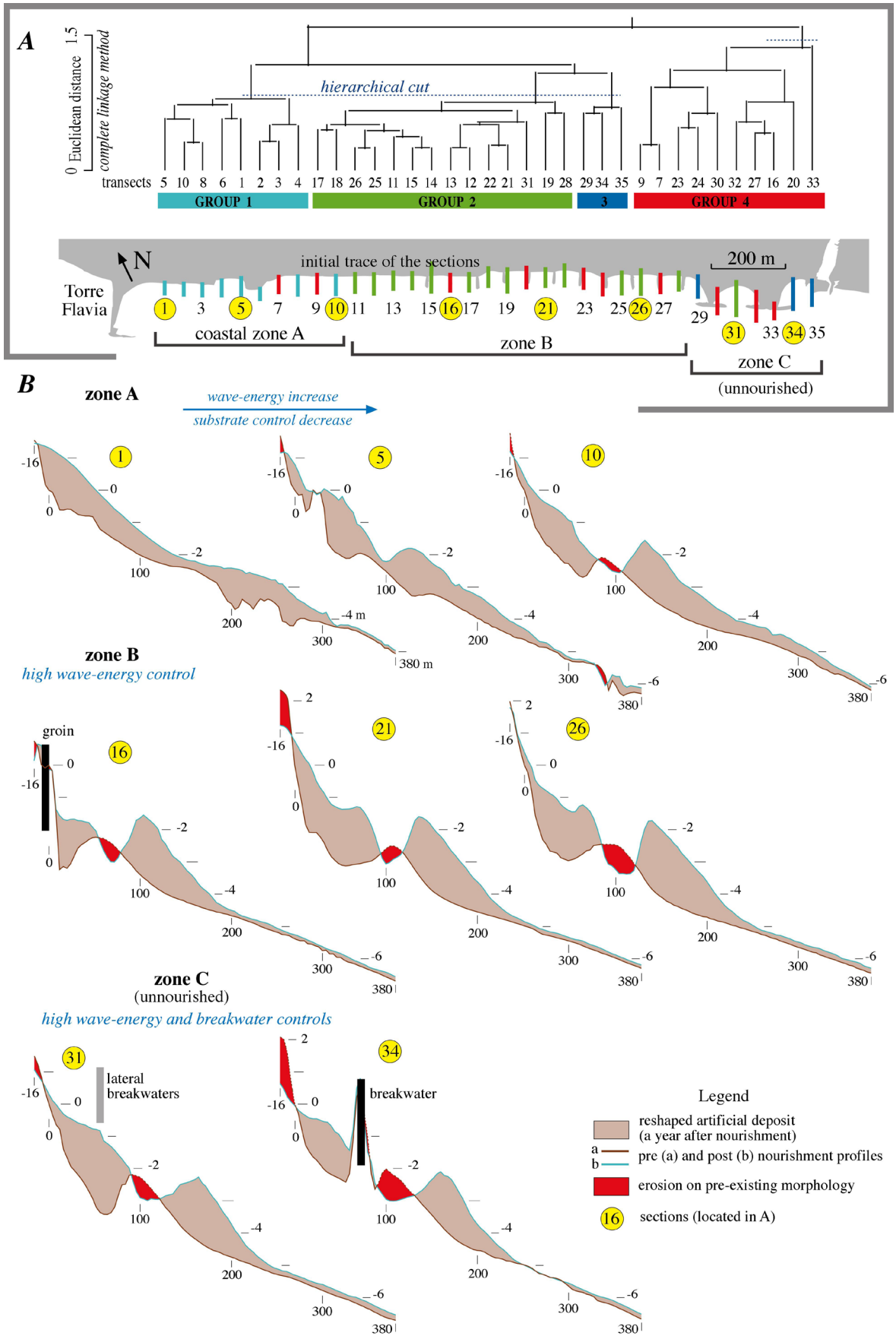

Fig. 2 - Recurring geometries of the artificial deposit. In A, results of a cluster analysis based on thickness data of 35 cross-shore sections of the reshaped artificial deposit. The resulting groups of deposit sections identify three coastal zones with relatively uniform geometries, summarised by the representative examples in B.

In coastal zone B, the two sedimentary bodies are present throughout, with the external body well-developed due to the high wave energy that led to its formation (Fig. 2B: sections 21 and 26). The deposit sections with anomalous characteristics are those intercepting or passing very close to the groin structures, and are distinguished by the modest size of the inner body at shallow depths (Fig. 2B: section 16).

In coastal zone C, which was not directly nourished, the artificial deposit is still present with characteristics depending mostly on interference due to the two breakwaters (Fig. 2B: sections 31 and 34). Variations in geometry regard mainly the inner body, whereas the outer body is consistently well-developed.

3.3. DEPTH OF CLOSURE

Depth of closure (DoC) is a theoretical concept that concerns a wide range of topics, including the identification of the active zone for beach nourishment designs (Hinton and Nicholls, 1998; Nicholls et al., 1998; Phillips and Williams, 2007; Aragones et al., 2018; Valiente et al., 2019). The depth of closure here is estimated through three different approaches, based on wave parameters, morphological features, and sedimentological evidence.

The first approach uses wave parameters calculated from climate data in Tortora (2020, part 1 in this volume), and takes two DoCs into consideration. The inner DoC (d_L *sensu lato*) marks the seaward limit of the zone along which bed stresses by waves are relevant, and seafloor topography changes significantly over time. The outer DoC (d_i), instead, identifies the seaward limit of a more external zone, where wave shoaling is the dominant process and topographic changes are negligible over time. This approach uses the equations below to estimate the inner DoCs according to Hallermeier (1978, 1981) and Birkemeier (1985), d_{LH} and d_{LB} respectively, and the outer DoC (d_i) by Hallermeier method (1978, 1981):

(1) $d_{LH} = 2.28\ H_e - 68.5\ (H_e^2/ gT_e^2)$
(2) $d_{LB} = 1.75\ H_e - 57.9\ (H_e^2/ gT_e^2)$
(3) $d_i = (H_{sm} - 0.3\ \sigma_s)\ T_{sm}\ (g/5000D)^{0.5}$

where: H_e (estimated at 3.38 m) is the effective wave height; T_e (= 6.68 sec) is the associated wave period; g = acceleration due to gravity; H_{sm} (=0.70 m) is the yearly median significant wave height, and σ_s (=0.558) is the related standard deviation; T_{sm} (=3.68 sec) corresponds to the wave period associated to H_{sm}; and D (=0.1 mm) is the sediment D_{50} at a depth of about 1.5 times greater than the inner DoC. The DoCs obtained from these equations are: d_{LH}=6.54 m (equation 1); d_{LB}=4.85 m (2); d_i=8.81 m (3). The different values of the two inner DoCs fall within the norm, since equation 1 generally provides closure depths greater than 20-30% when compared to equation 2.

The second approach identifies the inner DoC as the shallowest depth where no significant changes in bottom elevation occur over time (Krauss et al., 1998; Hartman and Kennedy, 2016). In the studied case, this is the depth at the external pinch-out of the artificial deposit. Figure 3A shows the pinch-out depths detected along 92 cross-shore sections of this deposit. Excluding the zone where the substrate control is high and the pinch-out is additionally affected by scattered rocky outcrops, the inner DoC falls in the depth range of 4.5-5 m, and tends to increase eastward with coastal exposure.

The third approach is based on the cross-shore distribution of six size intervals (families) of environmental significance (Tortora, 2020, part 1 in this volume: see Fig. 7). Figure 3B shows their variations (%) in pre-fill (sampling of 06.2001) and post-fill (06.2005) stages along a composite sedimentological and morphological transect representing the entire coast. Excluding families F1, F5 and F6 with very low percentages, the inner DoC can be inferred by the cross-shore variations of family 2 (coarse-medium sandy interval). In fact, in both stages, this family is relegated landward the deposit pinch-out and in its proximity starts to be sharply absent (Fig. 3B). This evidence collocates the inner DoC at about 5 m. The outer DoC, of more uncertain identification, should be at about 8-9 m, where the percentages of F3 (fine and very fine sands) and partially F4 (coarse silt) become constant proceeding seaward. It should be noted that the inner DoCs estimated by the Birkemeier equation and the other two approaches practically coincide. This study uses as a general reference d_L=5 m.

4. EXPLORATION ON KEY ASPECTS

4.1. WAVE CLIMATE

The wave climate that presided over the artificial-deposit remoulding in the year following the intervention was reconstructed in order to ascertain eventual climatic anomalies potentially connected to the nourishment failure. Data processed are those recorded from the buoy off the Civitavecchia coast in the time interval of April 2003 - March 2004.

Data in figures 4A and C indicate that wave directions from the WSW (18%), S (13%), SW (12%), and SSE (10%) are the most frequent. Excluding calm seas (9%), the classes of significant wave height (H_s) with major recurrences are 0.25-0.75 m (54%), 0.75-1.25 m (18%), and 1.25-1.75 m (9%). The classes in the range of 1.75-3.25 m have an occurrence of 9%, whereas waves higher than 3.25 m are rare (0.7%) especially those related to major storm events (H_s>3.75 m: 0.19%). The most frequent classes of wave median period (T_m), in figure 4B, are 3-4 sec (35%), 4-5 sec (20%), 2-3 sec (15%), and 5-6 sec (14%). They are mainly associated with waves from the WSW, S, SW, and subordinately from the SSE and WNW.

Comparing this annual wave climate with that of the longer time series (04.2003-03.2014) in Tortora (2020, part 1 in this volume), it results that H_s and T_m classes have similar recurrences in these two periods (Fig. 4 D,E), although some differences are observed in the distribution of H_s classes by wave directions. Using the effective wave height (H_e) (i.e. average wave conditions

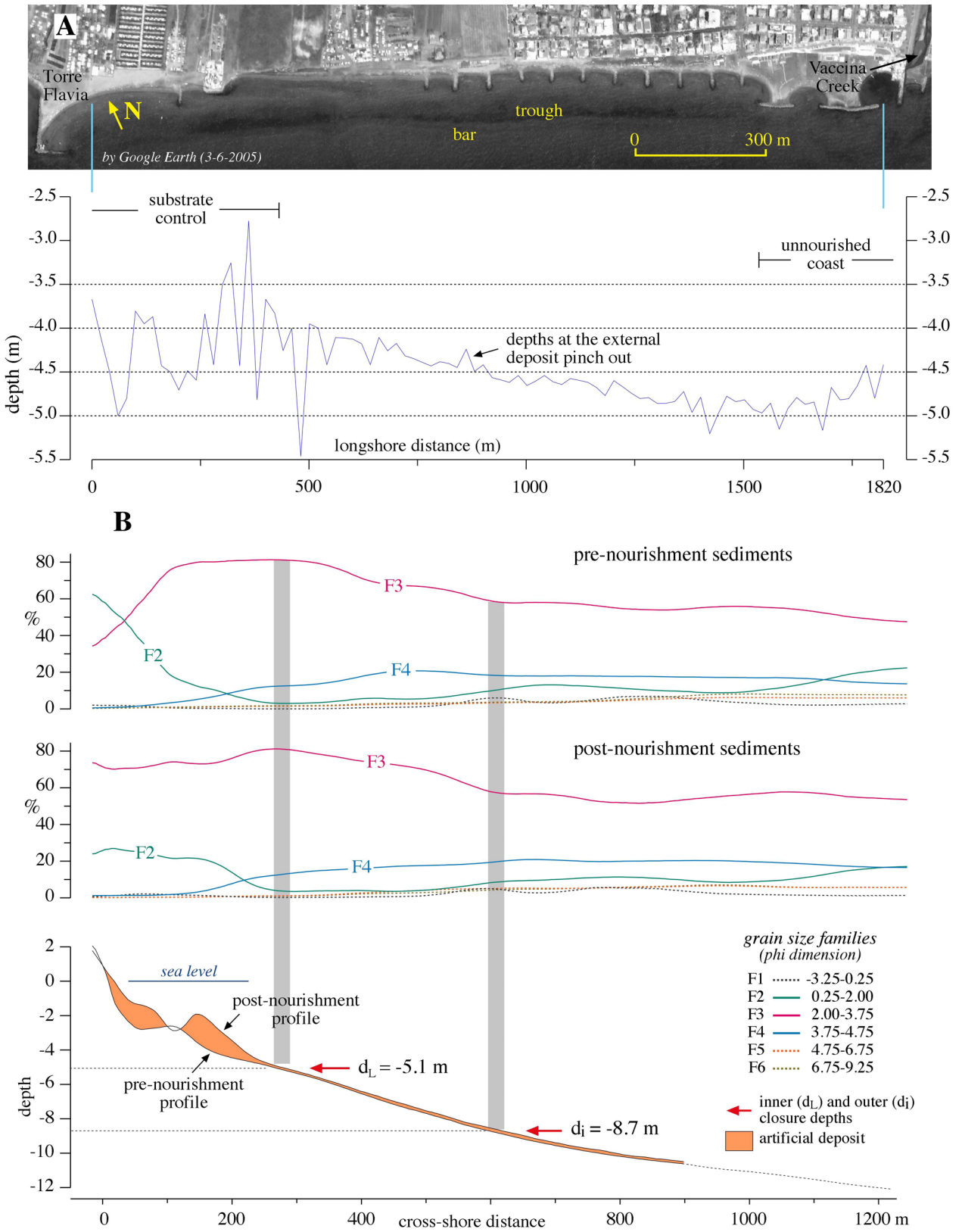

Fig. 3 - Identification of the depth of closure through morphological and sedimentological data. In A, the depth at the artificial deposit pinch-out is used to define the variations along coast of the inner closure depth (d_L). In B, inner and outer (d_i) closure depths are identified by the variations (%) of six size intervals (or families) along a composite cross-shore profile including pre-nourishment and post-nourishment data. The pattern of three size families (F2, F3, F4) localises d_L and d_i in the positions of the two bands in gray.

A

Directions/Hs classes (m)	0.25-0.75	0.75-1.25	1.25-1.75	1.75-2.25	2.25-2.75	2.75-3.25	3.25-3.75	3.75-4.25	>= 4.25	total %
348.75 - 11.25 (N)	0.999	0.504	0.033	0.000	0.000	0.000	0.000	0.000	0.000	1.535
11.25 - 33.75 (NNE)	0.594	0.058	0.000	0.000	0.000	0.000	0.000	0.000	0.000	0.652
33.75 - 56.25 (NE)	0.272	0.017	0.000	0.000	0.000	0.000	0.000	0.000	0.000	0.289
56.25 - 78.75 (ENE)	0.239	0.033	0.008	0.000	0.000	0.000	0.000	0.000	0.000	0.281
78.75 - 101.25 (E)	0.256	0.041	0.008	0.000	0.000	0.000	0.000	0.000	0.000	0.305
101.25 - 123.75 (ESE)	0.495	0.074	0.008	0.000	0.000	0.000	0.000	0.000	0.000	0.578
123.75 - 146.25 (SE)	3.079	0.693	0.173	0.050	0.050	0.000	0.000	0.000	0.000	4.045
146.25 - 168.75 (SSE)	4.565	2.534	1.717	0.528	0.578	0.107	0.000	0.000	0.000	10.030
168.75 - 191.25 (S)	7.892	2.741	1.280	0.495	0.132	0.000	0.000	0.000	0.000	12.539
191.25 - 213.75 (SSW)	6.315	1.032	0.537	0.421	0.008	0.000	0.000	0.000	0.000	8.313
213.75 - 236.25 (SW)	5.217	2.485	2.171	1.172	0.429	0.305	0.074	0.017	0.000	11.871
236.25 - 258.75 (WSW)	6.406	4.169	3.104	1.552	1.147	1.395	0.404	0.033	0.000	18.210
258.75 - 281.25 (W)	5.795	0.825	0.173	0.074	0.033	0.025	0.025	0.041	0.041	7.033
281.25 - 303.75 (WNW)	7.520	1.354	0.066	0.091	0.041	0.050	0.025	0.008	0.008	9.163
303.75 - 326.25 (NW)	3.236	0.504	0.008	0.000	0.000	0.000	0.000	0.000	0.000	3.748
326.25 - 348.75 (NNW)	1.552	0.553	0.000	0.008	0.000	0.000	0.000	0.000	0.000	2.113
Sub-Total	54.433	17.616	9.287	4.392	2.419	1.882	0.528	0.099	0.050	90.705
Calms (Hs < 0.25)										9.295
Total										100.000

B

Directions/Tm classes (sec)	0 - 2	2 - 3	3 - 4	4 - 5	5 - 6	6 - 7	7 - 8	8 - 9	>= 9	total %
348.75 - 11.25 (N)	0.000	0.438	0.693	0.132	0.173	0.033	0.025	0.008	0.033	1.535
11.25 - 33.75 (NNE)	0.000	0.380	0.099	0.041	0.058	0.017	0.008	0.000	0.050	0.652
33.75 - 56.25 (NE)	0.000	0.173	0.041	0.008	0.041	0.000	0.000	0.008	0.017	0.289
56.25 - 78.75 (ENE)	0.000	0.149	0.050	0.008	0.025	0.000	0.033	0.000	0.017	0.281
78.75 - 101.25 (E)	0.000	0.099	0.099	0.033	0.033	0.000	0.000	0.017	0.025	0.305
101.25 - 123.75 (ESE)	0.000	0.338	0.124	0.000	0.017	0.058	0.008	0.000	0.033	0.578
123.75 - 146.25 (SE)	0.000	1.956	1.346	0.264	0.198	0.124	0.099	0.025	0.033	4.045
146.25 - 168.75 (SSE)	0.000	2.031	3.607	2.237	1.535	0.322	0.116	0.083	0.099	10.030
168.75 - 191.25 (S)	0.000	1.032	5.357	2.930	2.039	0.792	0.289	0.083	0.017	12.539
191.25 - 213.75 (SSW)	0.000	0.553	3.657	2.410	1.197	0.338	0.107	0.033	0.017	8.313
213.75 - 236.25 (SW)	0.000	0.504	4.119	4.020	2.476	0.603	0.058	0.041	0.050	11.871
236.25 - 258.75 (WSW)	0.000	0.809	4.260	5.911	4.912	2.055	0.165	0.041	0.058	18.210
258.75 - 281.25 (W)	0.000	1.626	3.599	0.892	0.446	0.248	0.091	0.083	0.050	7.033
281.25 - 303.75 (WNW)	0.000	2.543	5.035	0.578	0.644	0.182	0.107	0.017	0.058	9.163
303.75 - 326.25 (NW)	0.000	1.362	1.767	0.116	0.215	0.132	0.083	0.041	0.033	3.748
326.25 - 348.75 (NNW)	0.000	0.875	0.842	0.091	0.157	0.058	0.008	0.033	0.050	2.113
Sub-Total	0.000	14.867	34.695	19.671	14.165	4.961	1.197	0.512	0.636	90.705
Calms (referred to Hs)										9.295
Total										100.000

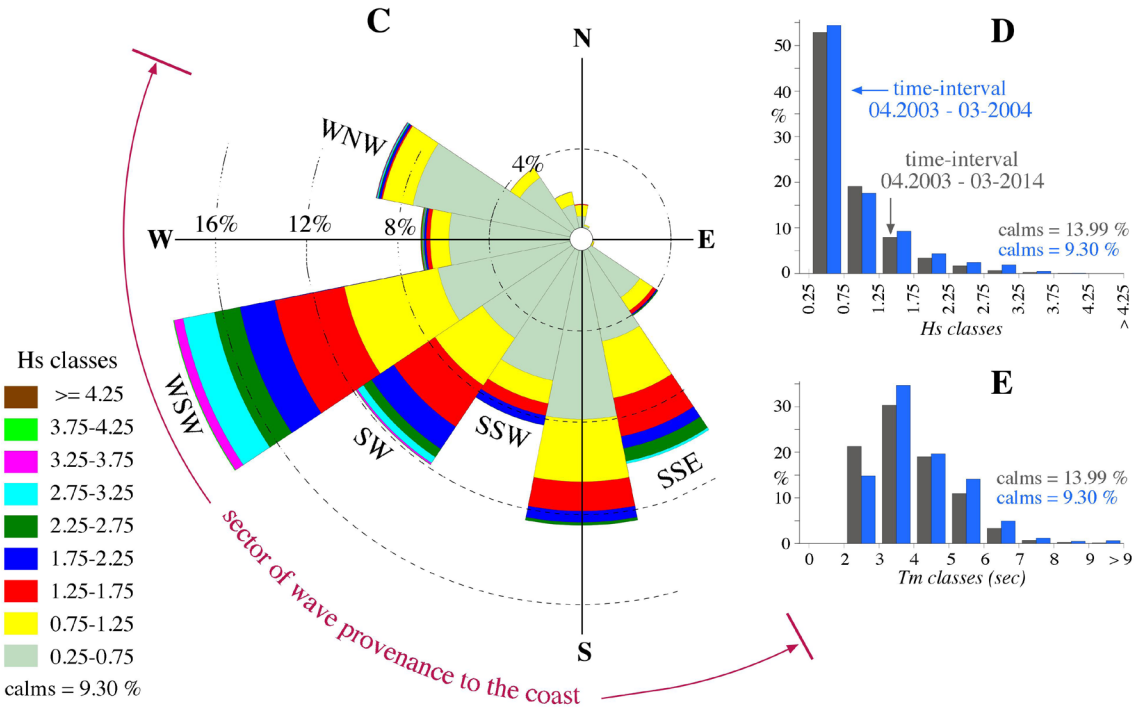

Fig. 4 - Wave climate in the period of the artificial deposit reshaping (data from March 2003 - April 2004). The matrixes in A and B refer to the recurrences (%) by wave directions of the significant wave height (Hs) and wave median period (Tm), respectively. Diagrams in C, D, E, summarize the information in these two matrices. Wave data of a longer period (2003-2014) are also reported for comparison in D and E.

exceeding only 12 hours out of a year; Hallermeier, 1978) and the associated wave period (T_e) as descriptors of extreme events, no significant differences appear between annual period (H_e=4.2 m, T_e=6.5 sec) and longer period (H_e=3.8 m, T_e=6.83 sec). The compared data indicate that the artificial deposit reshaping did not occur in anomalous climate conditions.

4.2. BORROW AND NATIVE SANDS

The nourishment sands were mined off the Capo d'Anzio coast (75 km southeast of Ladispoli Beach) from the upper portion of an extensive marine deposit of the last post-glacial transgression (Regione Lazio, 2003). The cores from this deposit portion show fairly constant stratigraphic characteristics and, beneath a superficial thin layer with modern palimpsest sediments (a mixture of sand, mud and biogenic detritus), comprise of well-sorted fine sands (Wentworth, 1922; Folk and Ward, 1957) ranging between three size (D_{50}) intervals (Fig. 5A): 0.15-0.175 mm (cores: V02_A3, V02_A4, V02_A5), 0.175-0.2 mm (V02_A2, A99) and 0.2-0.225 mm (V02_A4, A8). Before nourishment, sediments with these dimensions (0.15-0.225 mm) were present at shallow depths along the Ladispoli coast (Fig. 5B).

Figure 5C shows the average grain size characteristics of the sands in the cores and of the native sediments present in the beach-shoreface zone of the project site. The composite borrow sand (of all cores) is equal in size (D_{50}) and better sorted than the native sediment, showing particles mainly concentrated (80%) in the fraction 2-3 phi (0.250-0.125 mm). Overlaying the two granulometric curves (Fig. 5C; box on the left), this sand is greatly increased (+38%) in particles on the central part of the curve, whereas deficits are present on the right (-26%) and left (-12%) tails.

These granulometric differences were assessed by sedimentological methods typically used in nourishment design. One method is the stability index (Pranzini, 1999; Pranzini et al., 2018) that compares the two grain-size frequency distributions, with a resulting value of 1 meaning maximum stability of the borrow sand, zero meaning total instability, and approaching 0.5 as the stability of two sediments becomes more similar, as in this specific case (0.46). The overfill factor (James, 1975; Hobson 1977), in contrast, does not provide solutions since the borrow sand is better sorted than native sediment, and is therefore not transformable in this sediment according to the theoretical assumptions of the method. If the two grain-size frequency distributions are compared fraction by fraction (Krumbein and James (1965), the greatest deficit of the borrow sand falls within the size interval of 1-2 phi. Finally, the renourishment factor (James, 1974; 1975) predicts that in conditions of a negative sediment budget the removal rates of the borrow sand and native sediment are at ratio 1.5:1.

4.3. PROFILE EVOLUTION SCHEMES

These schemes are here applied to a composite section of the reshaped artificial deposit that represents morphological and sedimentological features in zone B (Fig. 2). This zone has been selected because is laterally well extended and, at the same time, is characterized by deposits with relatively constant geometries and by low influences from substrate and coastal structures.

4.3.1. Equilibrium beach-profile method

Without the use of any form of prediction, the concept of equilibrium beach profile (EBP) has been used as a theoretical support to subdivide the artificial deposit into elementary portions of environmental significance (Pilkey et al., 1993; Dean, 2002). Figure 6A shows the pre-nourishment and post-nourishment profiles (R1 and R2) and their morphologic simplification (P1 and P2), resulting from a best-fitting process by the EBP equation ($h=Ay^m$, m=0.67; Dean 1991), in which the sediment scale parameter "A" and profile shape factor "m" have been left as undefined variables. This process assigns to P1 and P2 profiles m=0.45 and m=0.68, respectively. Compared to the shape of an EBP (m=0.67), P1 exhibits excess in concavity and then in sediment accommodation space (positive), whereas profile P2 is an EBP. This positive space is quantified by sediment volume "a", enveloped between P1 and its expression in an equilibrium condition, such as profile P3. Similarly, this last profile was generated through a best-fit process (on R1 data), in this case setting "m" at a value of 0.67 (i.e. the shape factor for the equilibrium). Finally, according to methodology in USACE (2008), the shift of P2 on the pre-nourishment shoreline originates profile P4 that identifies volumes "b" and "c".

The three deposit portions (a, b and c) correspond to the sediment amounts engaged to fill the concavity excess in profile P1 (a=56 m^3/m), to equilibrate profile P4 (a+b=161 m^3/m), and to promote sediment progradation and shoreline advance (c=51 m^3/m). Of note is the relevant disproportion between the volume consumed for profile equilibration (161 m^3/m), and that used for profile progradation (only 51 m^3/m).

4.3.2. Depositional tendency of the borrow sands

According to Guillen and Hoekstra (1996) and to the null-point theory (Cornaglia, 1989; Bowen, 1980; French, 2005), nourishment deposition should follow a principle of "grain size similarity", in reference to which sediment accumulation preferentially occurs at depths where local sediments are as similar as possible to the fill sand. Data in figure 6B aim to validated this principle for the Ladispoli case upon the occurrence of the following condition: borrow sand that is very rich in the fraction 2-3 phi (80%) tends to be deposited in zones where this fraction abounded before nourishment. Such a condition was ascertained using (i) the smoothed pre-fill (P1) and post-fill (P2) shoreface profiles (already illustrated in figure 6A), (ii) the horizontal distances (translations) between these profiles at each minimized depth interval, and (iii) the corresponding percentages (%) of the native fine sand fraction (2-3 phi) along shoreface P1 (Fig. 6B). It should

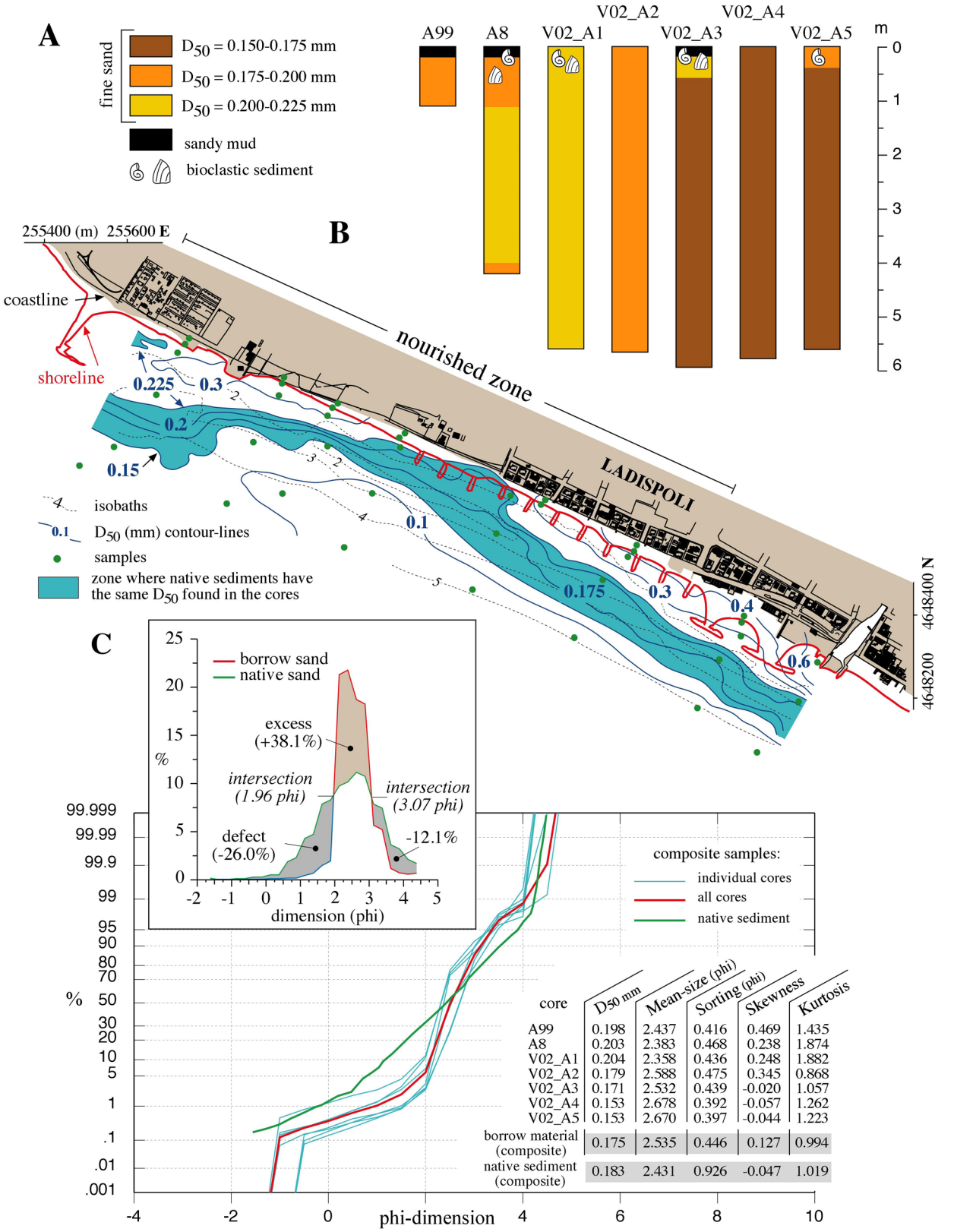

core	D50 mm	Mean-size (phi)	Sorting (phi)	Skewness	Kurtosis
A99	0.198	2.437	0.416	0.469	1.435
A8	0.203	2.383	0.468	0.238	1.874
V02_A1	0.204	2.358	0.436	0.248	1.882
V02_A2	0.179	2.588	0.475	0.345	0.868
V02_A3	0.171	2.532	0.439	-0.020	1.057
V02_A4	0.153	2.678	0.392	-0.057	1.262
V02_A5	0.153	2.670	0.397	-0.044	1.223
borrow material (composite)	0.175	2.535	0.446	0.127	0.994
native sediment (composite)	0.183	2.431	0.926	-0.047	1.019

Fig. 5 - In A, grain size characteristics (D_{50}) of the cores collected in the marine area of sand extraction. In B, distribution along the Ladispoli coast of the sediment D_{50} parameter in the pre-nourishment period, with distinction of the zone (in colour) enclosing the same D_{50} values found in the cores. In C, composite granulometric data related to borrow sands in each core and all cores, and to the native beach-shoreface sands in the nourished zone (statistical indexes according to Folk and Ward, 1957); in the box, the last two composite sands are visually compared.

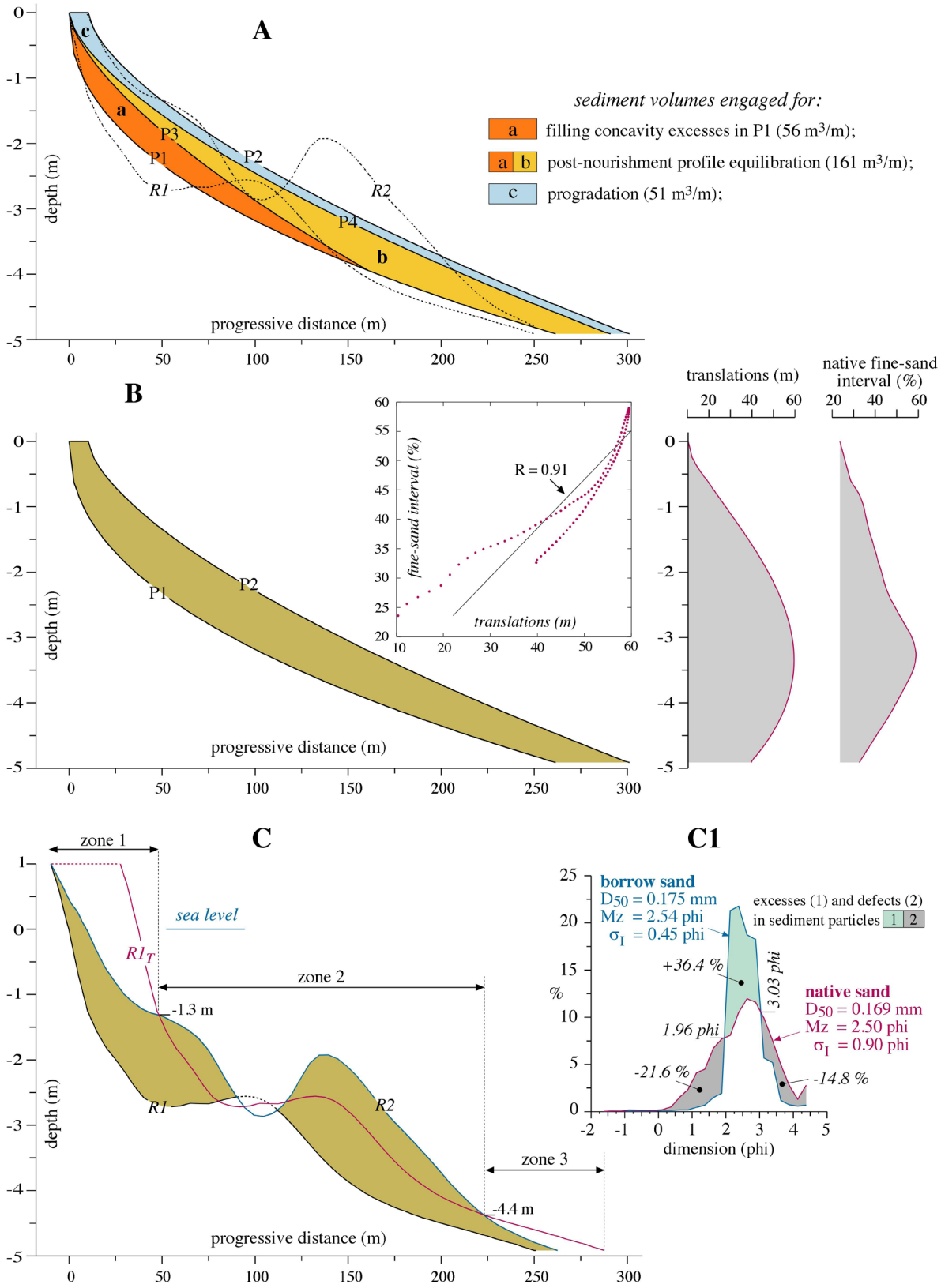

Fig. 6 - Reconstructions applied on a composite section of the reshaped artificial deposit. In A, subdivision of this deposit into significant portions: P1 (R=0.97) and P2 (R=0.94) profiles originate by best-fitting processes on real R1 and R2 shorefaces; P3 (R=0.92) simplifies R1 in equilibrium condition; P4 is the shift of P2 on pre-nourishment shoreline. In B, the horizontal distances (translations) between pre-nourishment (P1) and post-nourishment (P2) shorefaces (already shown in A) are correlated with the contents (%) of native fine-sand fraction (2-3 phi) along shoreface P1. In C and C1, the differences between profile shape attributes (R1T and R2, with R1T=R1) and between sediment characteristics (borrow and native sands) are compared. Three size intervals (<2 phi, 2-3 phi; >3 phi) control morphological effects in distinct zones (zones 1, 2, 3, respectively).

be noted that translations (fill sand deposition) increase linearly (R=0.91) with the contents of this fraction (with the degree of similarity) along pre-fill shoreface, as the aforementioned principle states.

4.3.3. Relationship between sediment and profile-shape

This relationship is extrapolated by coupling the differences in shape between pre-nourishment (R1) and post-nourishment (R2) profiles, with the granulometric differences between borrow (B) and native (N) sands. The visual appreciation of the first differences requires the preliminary translation of R1 in position R1T, so that volumes between R1-R2 and R1-R1T are balanced (Fig. 6C). This reconstruction corresponds to an idealised nourishment by a material B=N (Dean, 2002), or to a natural progradation by local sediments (N). The overlap of R1T (=R1 in shape) with R2 identifies three distinct zones (zones 1, 2, 3) where the two profiles do not coincide.

In contrast, observing the granulometric differences between the two sands (Fig. 6C1), the most reasonable linkage is that size intervals <2 phi, 2-3 phi and >3 phi preside over the morphological effects in zone 1, 2, and 3 respectively, that is, where the three intervals have their optimal residence (for the interval 2-3 phi, see figure 6A). Therefore, compared to sand N (or to a natural episode of progradation), the material used at Ladispoli Beach undernourishes internal and external profile segments (zones 1 and 3) due to its paucity in coarse (<2 phi) and fine fractions (>3 phi), and excessively feeds the middle profile portion (zone 2) due to the overabundance of medium-sized fractions (2-3 phi).

4.4. SHOREFACE SEDIMENT ACCOMMODATION SPACE

Based on the procedures in Section 4.3.1., 46 cross-shore transects have been considered calculating for each: (i) the profile shape factor (m) of pre-fill and post-fill shorefaces (in reference to figure 6A, P1 and P2 profiles), (ii) the volumes contained within the concavity excesses (Fig. 6A: volume "a") or concavity defects (volume "a" when P1 lies above P3) of the pre-nourishment shoreface, and (iii) the depth where these volumes run out (figure 6A: the external intersection of P3-P1 profiles). Figure 7 shows the variations of these parameters along the coast, synthesized as follows:

- Pre-nourishment shorefaces exhibit mainly excesses in concavity (on average, m=0.52; Std Deviation=0.143), whereas the post-nourishment shorefaces often show a moderate flattening (western coast), or shapes near or coincident to the equilibrium (m=0.69; Std Deviation= 0.109) (Fig. 7A).

- Volumes contained within excesses or defects in concavity in the entire investigated area amount to 79,350 m^3 and 6,170 m^3, and in the nourished zone to 72,690 m^3 and 2,450 m^3 (Fig. 7B).

- These volumes reside between the shoreline and 3.8-4.0 m depth, in reference to the pre-fill bathymetry (Fig. 7C), extending over most of the shoreface length.

Note the relevant sand volume within the above-mentioned concavity excesses, corresponding in the nourished zone to 20% of the artificial deposit volume (372,380 m^3; Fig. 8C).

4.5. SEDIMENT LOST FROM THE PROJECT SITE

Any nourished beach experiences a tendency to expel the sediment overabundance beyond the boundaries of the project site, resulting in sand loss and reduction in nourishment performance (Elko et al., 2005; De Schipper et al., 2016; Marinho et al., 2018; Spodar et al., 2018). At Ladispoli Beach, these losses have been estimated as the imbalance in the artificial deposit volume between two stages. The first stage concerns the short time of the nourishment operations (1-2 months), during which natural sediment redistribution was not completely absent. In fact, the classes of significant wave height <0.25 m, 0.25-1 m, 1-2 m, and 2-3 m had recurrences of 7.1 %, 76.2 %, 15.3 % and 1.4 %, respectively (data from March-April 2003). Moderate wave activity is also suggested by the fairly regular prismatic geometry of the underwater artificial deposit. The second stage extends over the following year, during which expulsion of the sediment overabundance is a typical phenomenon.

Figure 8 summarizes the results of volumetric estimates that, based on grid data of two isopach maps (one per stage) of the artificial deposit (Tortora, 2020, in this volume), have considered the investigated area and its two component sub-areas (1 and 2). Focusing on sub-area 1, the one directly nourished, data in figure 8C highlight the following aspects: (1) the nourishment was supported by native fine sands (44,680 m^3) which have been recovered by erosion on pre-existing morphology during both stages (Fig. 8 A,B); (2) those recovered in stage 1 (25,090 m^3), within a system supposedly closed due to the brevity of this stage, were likely incorporated into the artificial deposit (421,140 m^3), and its net volume (396,050 m^3) then refers to the sediment amount used for the intervention; (3) the negative sediment imbalance resulting between the two stages (-48,760 m^3) corresponds to the sediments lost from the project site (sub-area 1); (4) these sediments accumulated in the unnourished sub-area 2 (Fig. 2B: profiles 31, 34), with a positive imbalance (+36,910 m^3), and further to the east (Fig. 9A, profile P19); (5) the sediments lost correspond to 12% of the initial artificial deposit volume (stage 1), a quantity within the normal range of most nourishment interventions (Verhagen, 1996).

5. VIRTUAL NOURISHMENT AND DIAGNOSTIC TESTS

The nourishment has been virtually reproduced and then explored through the Grain-size Nourishment Model (GNM; Tortora, 2008), a program which, when provided with given topo-bathymetric and granulometric information describing the pre-fill profile, returns the morphologic evolution according to pre-

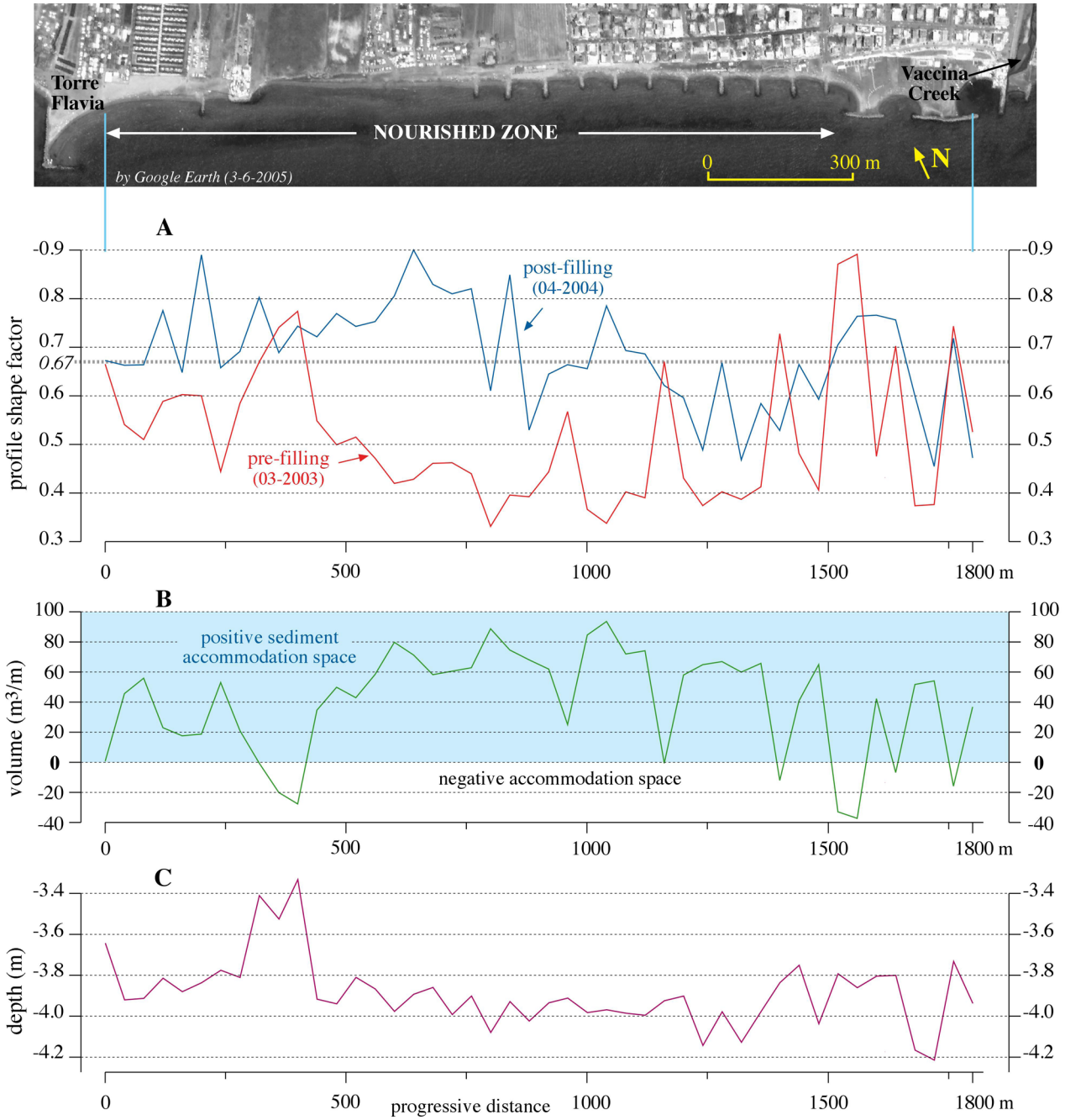

Fig. 7 - Variations along the coast of different parameters: the profile shape factor related to pre-and post-nourishment shoreface profiles (in A); the amounts (m^3) of positive and negative sediment accommodation space, corresponding to the excesses and defects in concavity along pre-fill shoreface topography (in B); the maximum depth delimiting the zones with positive and negative accommodation spaces (in C).

selected nourishment variables (profile boundaries, input volume and grain size characteristics of the borrow sand). The model was preliminarily tested on the full investigated area by comparing its outputs with real post-nourishment features (Fig. 9). After visual validation, a "composite simulation" was performed using the input data of the individual reproductions (in particular, P13, P14, P15 and P16; Fig. 9A). This composite simulation, in figure 10A, intends to represent nourishment effects over a fairly large area (*i.e.* the previously selected zone B; Fig. 2), and was used as an exploration tool in the tests presented in the next sections. Some details on GNM and on the techniques adopted are given in Section 2.

5.1. ROLE OF SEDIMENT SORTING

Given that borrow and native sands differ mainly in sediment sorting, the role of this parameter (σ_I) has been evaluated by applying the composite simulation to some types of hypothetical borrow sands. These sands, all log-normal and with the same mean size of the borrow material used at Ladispoli, vary in σ_I from very well sorted (sand A) to poorly sorted (D) (Fig. 10B). The four

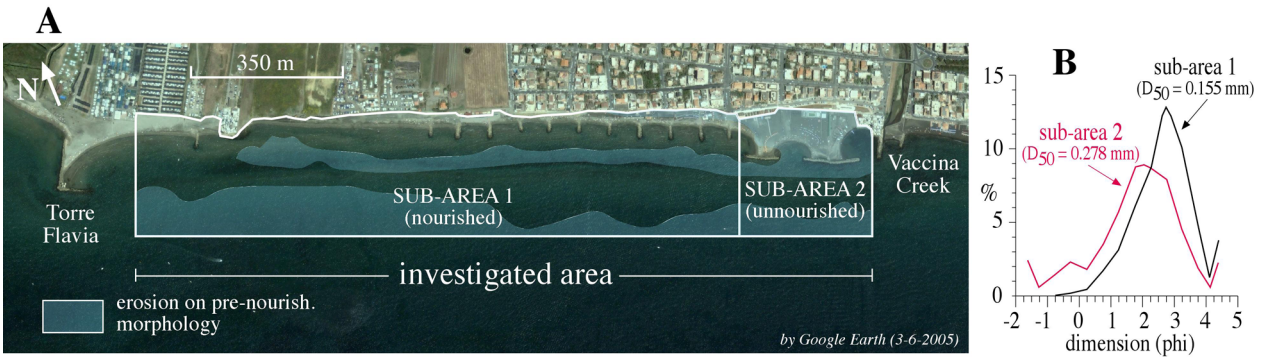

C

	sub-area 1 (volumes)			sub-area 2 (volumes)			whole investigated area (volumes)		
artificial deposit	*deposition*	*erosion*	*net vol.*	*deposition*	*erosion*	*net vol.*	*deposition*	*erosion*	*net vol.*
stage 1	421,140	25,090	396,050	17,370	14,980	2,390	438,510	40,070	398,440
stage 2	372,380	19,590	352,790	54,270	5,400	48,870	426,650	24,990	401,660
volumetric imbalance	-48,760	-5,500	-43,260	+36,910	-9,580	+46,480	-11,860	-15,080	+3,220
total erosion	/	44,680	/	/	20,380	/	/	65,060	/

deposition: amount of sediment deposition (artificial deposit volume)
erosion: amount of erosion on pre-nourishment morphology
net vol: differences between deposition and erosion amounts

Fig. 8 - Estimates of the artificial deposit volume at the end of the intervention (stage 1) and a year later (stage 2) are reported in this figure. In A, map showing the areas related to these estimates and the zones where pre-nourishment morphology was eroded in the total period of the two stages. In B, composite grain size distribution of the sediments eroded in the two sub-areas. In C, summary of the volumetric estimates; data in red refer to the net amounts of sediment lost (-) or gained (+) in sub-area 1 (directly nourished), sub-area 2, and in the complete investigated area.

sands generated very distinct evolutions. In fact, with the worsening of sediment sorting (from A to D sands), virtual deposition increases near and on the beach, and reversely decreases at the bar position (Fig. 10B). This test confirms the considerations related to figure 6C, and highlights an unexpectedly high correlation of the sediment sorting to nourishment performance. More generally, this test (and other simulations not reported here) indicates that a well-sorted sand tends to overfeed a distinct zone, whose position migrates landward with the increase of the sand size, and that this sand can even become highly performing (more than a normally sorted sediment) if, for example, similar in size to the sediments of the native dry beach. Unfortunately, this is not a case pertinent to the nourishment in question (Fig. 5B).

5.2. ALTERNATIVE BORROW SANDS

This test aims to assess the effects that would have been obtained at Ladispoli Beach using sands from alternative quarry areas. The sands tested by the composite simulation are those used for nourishing Fondi (sand A1) and Porto Badino (sand B1) beaches, and those (sands C1 and D1) of two potential marine quarry areas (areas 1-2 and 3, in Tortora, 1992) located to the east of Monte Argentario promontory (Fig. 10C). Virtual nourishments by sands A1, B1, and C1 provide relevant shoreline advances (47.5 m, 48.3 m, 43.9 m, respectively) that in the case of the two coarser sands (A1 and B1) are also accompanied by an increase in berm height (Fig. 10C). By contrast, fine sand D1 (D_{50}=0.124 mm) creates a submerged deposit and a narrow beach. The results above raise doubts about the choice of borrow sand used at Ladispoli Beach and, indirectly, suggest that no other factor caused the intervention to fail.

5.3. SEDIMENT PROGRADATION AND AGGRADATION COMPONENTS

In order to segregate these two components of sediment deposition, the composite simulation was performed using an alternative version of GNM, the Hybrid Grain-Nourishment Model (HGNM). In HGNM, two volumes (V_{pr}, V_{ag}) are assigned as input to separately predict the horizontal (V_{pr}) and vertical (V_{ag}) sediment accretions which, in pairs, recompose the depositional vectors that, anchored on the pre-fill profile, outline the predicted post-fill morphology. In this specific case, the final nourishment reproduction was obtained after numerous repetitions of the composite simulation, each for different combinations of V_{pr} and V_{ag} input volumes, until reaching the output that best imitated the real post-nourishment profile (*i.e.* the inverse method; Tarantola, 2005).

This output is the profile PL in figure 11A, and was obtained by input volumes of 145 m^3/m (V_{pr}) and 118 m^3/m (V_{ag}). As the result of the high V_{ag} volume, the depositional vectors generating profile PL are tilted by an angle of +0.8° with the horizontal (Fig. 11B). This angle corresponds to the average trajectory of the profile during virtual evolution and, theoretically, to the depositional

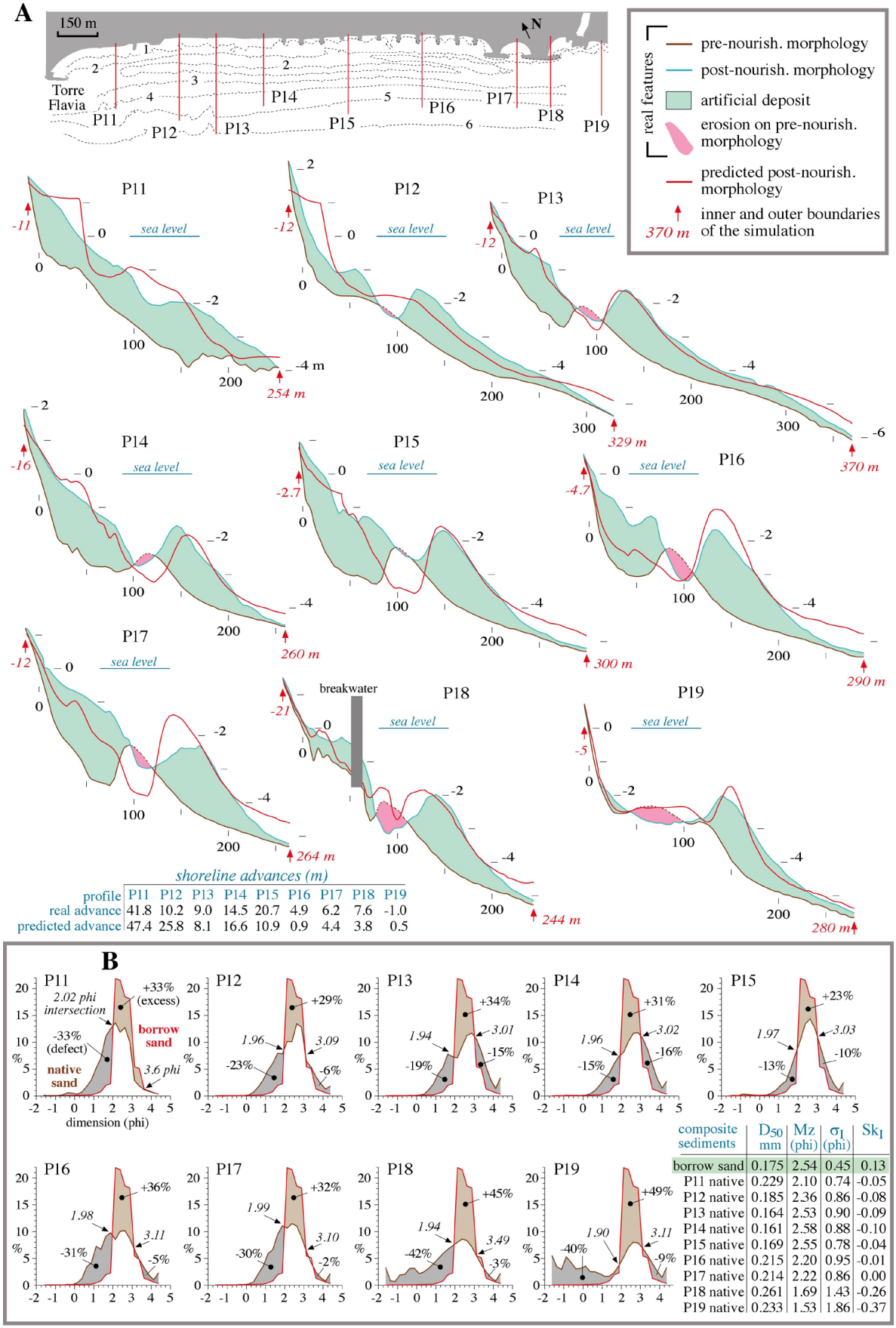

Fig. 9 - In A, visual comparisons between GNM predictions and real post-nourishment features. In B, grain size frequency distributions of the borrow material and the composite native sand representing the average sediment along each pre-nourishment profile.

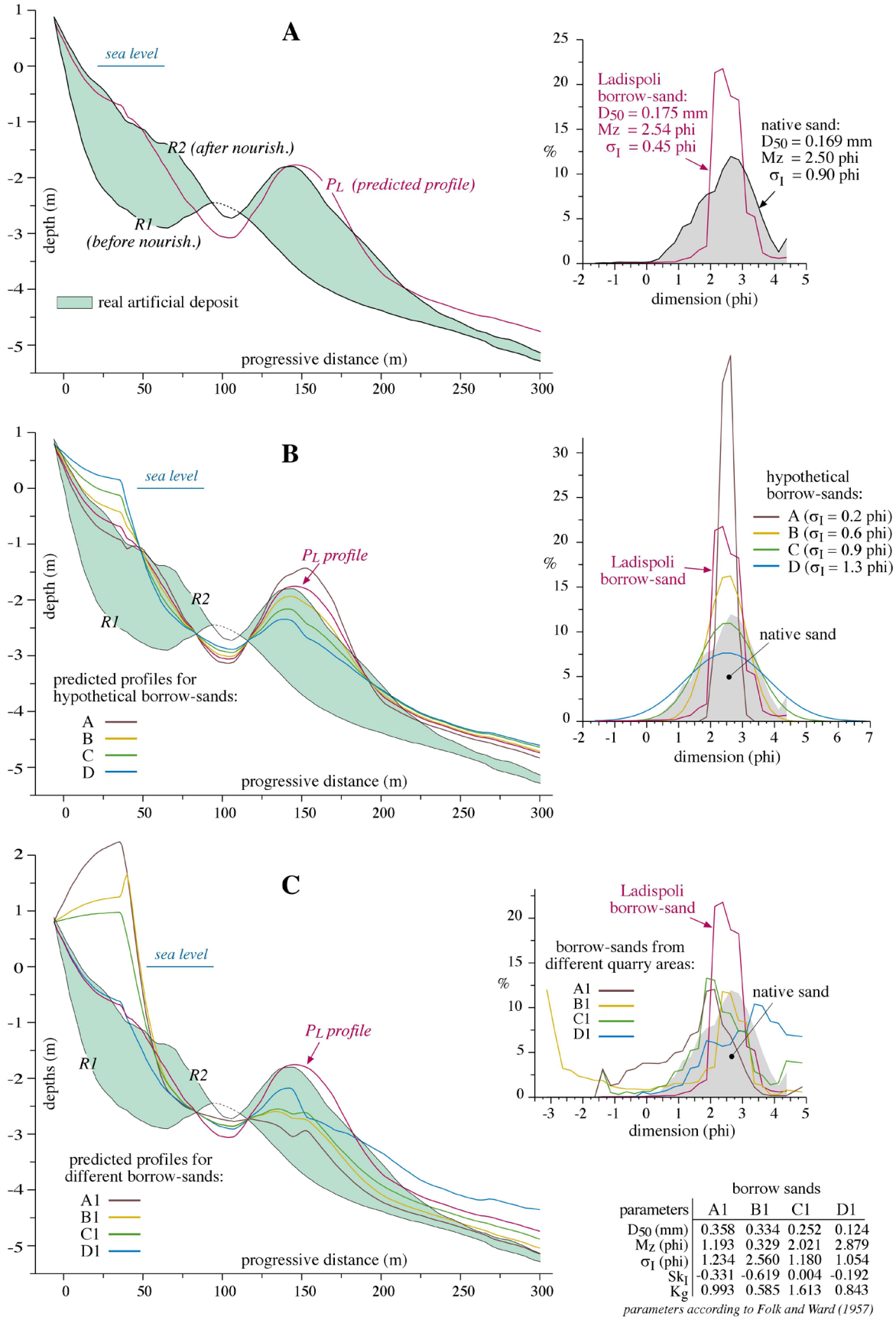

parameters	borrow sands A1	B1	C1	D1
D_{50} (mm)	0.358	0.334	0.252	0.124
Mz (phi)	1.193	0.329	2.021	2.879
σ_I (phi)	1.234	2.560	1.180	1.054
Sk_I	-0.331	-0.619	0.004	-0.192
Kg	0.993	0.585	1.613	0.843

parameters according to Folk and Ward (1957)

Fig. 10 - In A, the output (profile PL) of the "composite simulation" is validated through comparison with the real composite post-nourishment profile (R2); on the right side, the grain-size characteristics of native and borrow sands. In B, repetitions of this simulation by using four hypothetical borrow sands (on the right side, sands A to D) in order to ascertain the role of sediment sorting in the profile evolution. In C, further repetitions for alternative borrow-sand types (on the right side, sands A1 to D1).

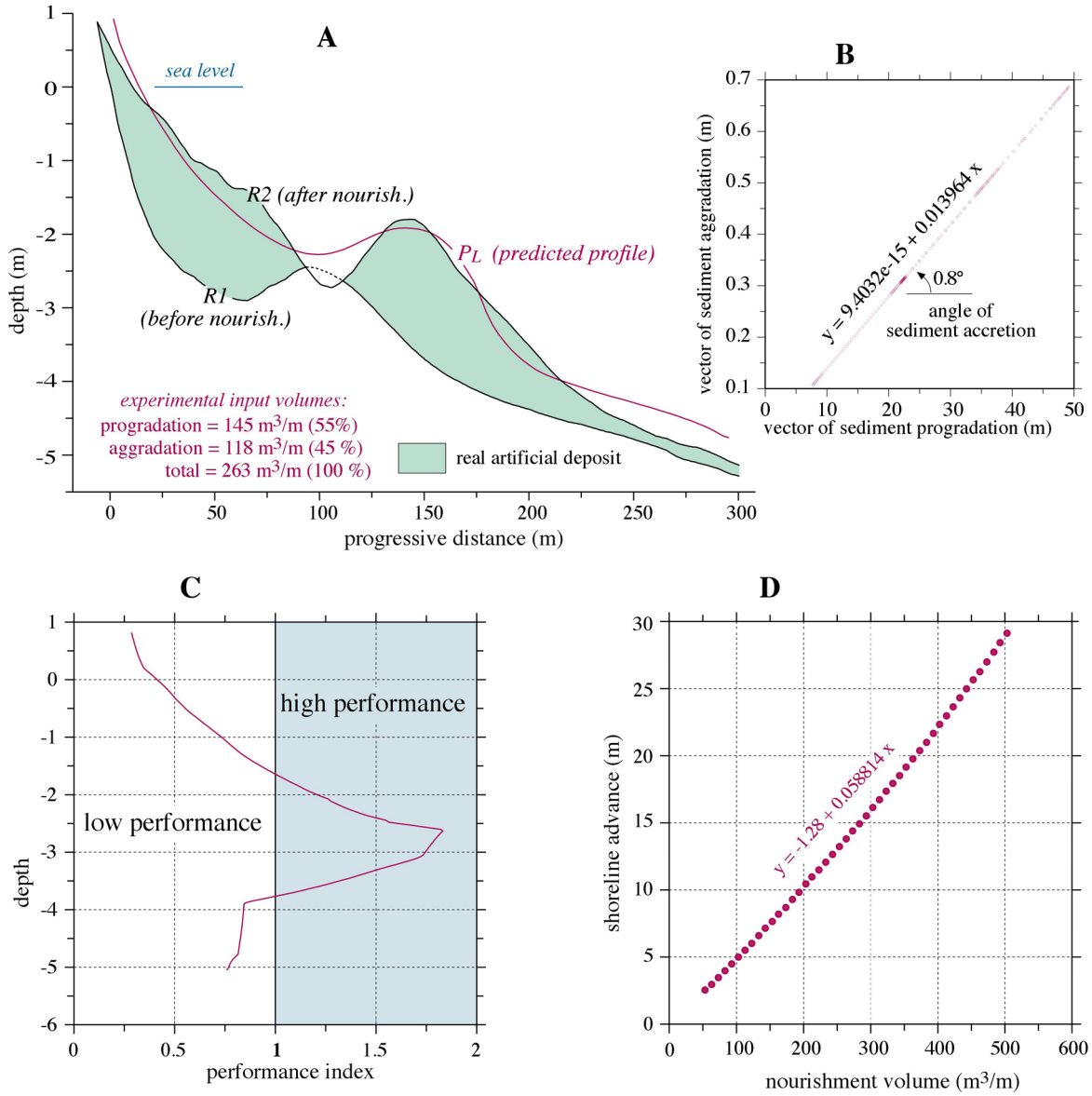

Fig. 11 - In A, imitation (PL profile) of the post-nourishment features (profile R2) through a volumetric calibration of the progradation and the aggradation components of virtual sediment deposition. In B, the pairs of horizontal and vertical vectors that originate profile PL define the orientation of the sediment growth. In C, variations with depths of performance index applied to the borrow sand used at Ladispoli Beach. In D, relationship between nourishment volumes and shoreline advances resulting from many repetitions of the simulation in A for different input volumes.

setting in the real artificial deposit (*sensu* Helland-Hansen and Martinsen, 1996; Tortora et al., 2009). The most relevant aspect in this nourishment imitation is the high amount of sands consumed for sediment aggradation (118 m^3/m) to the detriment of full progradational effects. Note also that only a small part of this amount (about 5%) is engaged in the vertical growth of the beach (10-15 cm).

5.4. BORROW SAND PERFORMANCE

Borrow sand performance was quantified through two different methodologies. One refers to the here called performance index (Pi), or the ratio, calculated at each depth interval of the pre-nourishment profile, between the translations (depositional vectors) respectively generated by the borrow and native sands. This method was applied to the input data of the composite simulation. The results are shown in the graph of figure 11C, in which values of Pi=1, Pi>1 and Pi<1 refer to depths where the performance of the nourishment sand is equal, higher and lower than that of the native sediment, respectively. In the graph, low and high performance values occur on the beach (on average, Pi=0.33) and at intermediate depths (Pi is up to 1.75), respectively. The Pi value at zero depth indicates that shoreline advances induced artificially (by borrow sand) and through natural progradation (by native sand), regardless of the amount of sediment supply, are at the ratio 0.41:1.

In the second method, here called shoreline index, the performance is instead expressed in absolute terms, as the sand volume required to promote 10 m of beach

widening. This index was calculated by coupling input (volume) and output (shoreline advance) data related to several repetitions of the composite HGNM simulation (Fig. 11A) keeping constant the ratio V_{pr}/V_{ag}. The linear equation resulting from the interpolation of these data pairs assigns an average of 191 m^3/m of sand as the shoreline index (to obtain 10 m of beach widening), a volume significantly greater than the norm (Fig. 11D).

5.5. SEDIMENT DEPRIVATION AND SHORELINE ADVANCE INHIBITION

As previously estimated in sections 4.4. and 4.5, the sediments lost from the project site amount to 34.8 m^3/m (*i.e.* the volumetric imbalance between the two stages in sub-area 1; Fig. 8C), which added to another 51.9 m^3/m of sand within the concavity excesses in pre-fill shoreface zones (Fig. 7B), make a total of 86.7 m^3/m. This is a fairly large sediment deprivation, equivalent to 29% of the initial artificial deposit volume. Evaluating its impact on the beach through the equation of figure 11D, it results unexpectedly very modest, corresponding to a missed shoreline advance of only 4 m. In contrast, some ad hoc simulations show that this impact is trebled (in terms of translation retention) on the middle profile segment, a zone with a high confluence of borrow sand and therefore more sensitive than the others to any variation in sediment supply. Overall, this sediment deprivation had a limited influence on nourishment performance.

6. DISCUSSION

6.1. INTEGRATION OF THE RESULTS

Table 1 shows the results of the main inspections performed in this study. Following the list of topics, the annual wave climate that presided over the remoulding of the nourished sand mass, because similar to the long-term climate, has no connection with the intervention failure (Table 1, point a). On the contrary, all sedimentological inspections demonstrate the inadequacy of the borrow sand to restore the Ladispoli Beach (Table 1, point b). This sand, equal in size to the native sediment but considerably better sorted, determines in negative sediment imbalance conditions removal rates which are predicted nearly equal (stability index; Pranzini et al., 2018) or 1.5 times greater (renourishment factor; James, 1975) compared to that of the native sediment. Further estimates indicate that, regardless of sediment input, shoreline advances by artificial (borrow sand) and natural (native sand) supplies are at the ratio 0.41:1, whereas sediment accretion rates (translations) average a ratio of 0.33:1 on the beach, reaching a ratio of up to 1.75:1 at depth interval 1.5-4 m (performance index). Moreover, the shoreline index signals the need for large quantities of this sand to promote beach widening. Ignoring the sand quality, the nourished volume complies with the objectives of the intervention.

In the borrow and native sands, the content (%) of three size intervals explains why post-fill and pre-fill profiles differ in shape and, ultimately, clarifies the sediment control on the growth of the artificial deposit. In particular, the shortage of coarse (<2 phi) and fine (> 3 phi) size intervals in the borrow sand is the cause of the deposit undergrowth on inner and outer zones, respectively (Table 1, point c). On the contrary, the huge deposition on the middle zone is due to the overabundance of medium-sized borrow particles (2-3 phi). Compared to the native sediment, the lack of coarse and medium sand fractions (<2 phi) corresponds in volume to 102,970 m^3. Therefore, about a quarter of the nourished volume lacks in particles normally present on the beach and very shallow seafloor. Overall, the deposit growth appears to be regulated by the tendency of the individual borrow fractions to settle at the depths of residence of the corresponding native sediment fractions.

Explorations inside the artificial deposit (Tab. 1, point c) suggest that a large part (76% in volume) of its submerged section includes sediments that have been involved in profile equilibration process without promoting progradational effects. A part of these sediments (26% of the submerged deposit volume), located above the lower deposit boundary, filled the concavity excess in pre-fill shoreface profiles, the latter degraded and in disequilibrium conditions. Virtual imitations of the nourishment highlight formative processes in which volumes engaged in the progradation and aggradation components of deposition are almost in the same proportions, with consequent retention in final nourishment progradation. Due to the aggrading component, the impulse of this progradation (the direction of deposit growth) is not aligned with the horizontal but inclined on average by an angle of +0.8°.

Despite the recovery of native sands (sediment gain) through erosion on pre-fill morphology, the sedimentary balance appears to be negative at the project site, mainly due to the sands transported laterally to the seabed of the adjacent east coast (Tab. 1, point d). Moreover, the sands within the concavity excesses of the pre-fill shoreface topography represent a further sediment subtraction for progradation (Tab. 1, point e). The total sediment deprivation, although relevant (29% of the initial artificial deposit volume), had a very limited impact on the beach and nourishment performance due to the too fine size of the sediments involved. About the pre-existing elements, the rocky bottom on the western border acted as a natural obstacle preventing the effects of lateral spreading on one side of the beach, whereas the groin system was ineffective in trapping nourishment sands (Tab. 1, point e).

Finally, three aspects deserve clarification. One aspect concerns the discrepancy found between D_{50} values and profile morphology, as highlighted by the fact that two sediments (native and borrow sands) with the same average size (Fig. 5C) are paradoxically related to two profiles of very different shape (the real pre-fill and post-fill profiles; Fig. 6A). This discrepancy depends on the information contained in the D_{50} parameter, which does not include details on those groups of fractions from which profile shape and nourishment outcomes are more

Tab. 1 - Summary of results of the inspections performed in the present study.

inspections	references in main text	comments
a) annual wave climate	4.1.	no out-of-ordinary wave conditions during reshaping of nourished sand mass
b) borrow sand:		
- average sediment size	4.2.	similar to the native sand ($D_{50} \simeq 0.18$ mm)
- sediment sorting	4.2.	significantly better sorted (σ_I=0.45 phi) than native sand (σ_I=0.92 phi)
- grain-size frequency distribution	4.2.	compared to the native sand, sediment overabundance (+ 38%) on the central part of the frequency curve (2-3 phi) and sediment lack on the left (-26%; <2 phi) and right (-12%;> 3 phi) tails.
- renourishment factor (James, 1975)	4.2.	less stability than native sand (R_J=1.5)
- stability index (Pranzini et al., 2018)	4.2.	slightly lower stability than native sand (Si=0.46)
- artificial and natural shoreline advances (by borrow and local sands)	5.4.	at the ratio 0.41:1
- performance index	5.4.	low performance for beach widening (on average Pi=0.33) and high in the middle profile portion (Pi up to 1.75)
- shoreline index	5.4.	high sediment quantities (191 m^3/m) to promote 10 m of shoreline advance
- sand volume	5.2.	complies with the objectives of the intervention
c) post-nourishment profile equilibration:		
- control of borrow-sands	4.3.3.	the abundance of size intervals <2 phi, 2-3 phi and >3 phi rules sediment deposition in inner, middle and outer profile portions, respectively
- sediment involved in profile equilibration (according to EBP method)	4.3.1.	76% of the volume of submerged artificial deposit (the remainder involved in the progradation)
- sediment aggradation and progradation components of deposition (according to HGNM reconstructions)	5.3.	equated in amount, with retention of profile translations due to the higher than normal aggradational component.
d) sediments lost and gained in the nourished zone during morphological adaptation:		
- net sediment imbalance	4.5.	-48,760 m^3 of sands, mainly accumulated beyond the eastern border in shallow depths
- sediments recovered by erosion on pre-fill morphology	4.5.	44,680 m^3 of fine and very fine native sands
- autochthonous sediment entering or exiting due to longshore drift		not estimated but probably in modest amounts
- nourishment benefits to adjacent beaches		none
e) pre-nourishment morphology:		
- shape of cross-shore profiles	4.4.	with excesses in concavity, filled by a large amounts of sand (72,690 m^3 in the nourished zone)
- elements counteracting lateral spreading	3.1.	pre-existing coastal structures (unable to trap the sands), and rocky bottoms at the western border (able to block longshore sediment transport)

directly dependent (Fig. 6C, C1). The predictive skills of this widely used parameter deserve attention because they may vary from case to case. In the Ladispoli case, for example, any method strictly based on this parameter would probably have led to incorrect morphological predictions. The second aspect regards the sediment composition, in particular the mineralogical contrast between borrow sands, essentially siliciclastic, and native sands which contain moderate quantities of heavy minerals that become clearly dominant on the beach. How much this contrast was assessed in the nourishment project, and how much it weighed into the final performance are points of possible relevance but not addressed in this study. The third aspect concerns the surplus of sediment for post-fill profile equilibration due to the excesses in water space (in shoreface concavity) in pre-nourishment morphology (Fig. 7). These space excesses, since in potential present in retreating coasts, should be assessed in advance with eventual counts of additional borrow sand amounts by way of compensation.

6.2. SEDIMENTARY PROCESS

The deposit formed by nourishment was the result of erosion and external redistribution of a part of the sand mass originally placed on the beach and very shallow seabed (Fig. 12). This dynamic was regulated by the

availability of water space for deposition, particularly by the geometric relationships between pre-fill morphology and profiles with shapes imposed by the borrow sand grain-size characteristics (Cowell and Kinsela, 2018). The needed space was found through a general shift of deposition to relatively deep water, and through distinct adaptation processes varying from zone to zone. In zones with negative accommodation space pre-fill morphology was eroded, deeply along the belt of migration of the bar trough, and more superficially in some scattered sectors. Whatever the cause, erosion also occurred during the period of nourishment operations, even in external areas. By contrast, in zones with positive accommodation space and high sediment confluence, once deposition reached the zero accommodation threshold (= sediment bypass), the incoming sediments began to flow directly out of the system. This dynamic occurred throughout the lateral extent of the outer sedimentary body (Fig. 12B) and was partially replaced on the western margin by some local seafloor collapses with consequent sediment transport by gravity beyond the inner closure depth (Tortora, 2020, Part 1 in this volume). A separate case concerns the steep pre-fill shoreface topography that was artificially filled during nourishment works. Changes in nearshore water circulation and wave impact on the shore should have occurred considering the different extent and depth of the breaking zone in pre-fill and post-fill periods (Fig. 12). It should be noted that little or nothing would probably have changed within the project site boundaries in case of a hypothetical increase in nourishment volume. The replication of the dynamics mentioned above would have led to an insignificant shoreline advance and an aggravation of the sediment losses due to the persistence of the sediment bypass along the outer sedimentary body. Even in nourishment simulations there is no possibility of achieving acceptable performances unless changing the type of fill sand.

7. CONCLUSION

The nourishment at Ladispoli Beach was an attempt to reintroduce the amount of sand lost during the erosive phase that started around 1960. This nourishment took place in a coast already protected by man-made structures, well delimited on the western side by raised rocky bottoms, and characterized by a steep shoreface

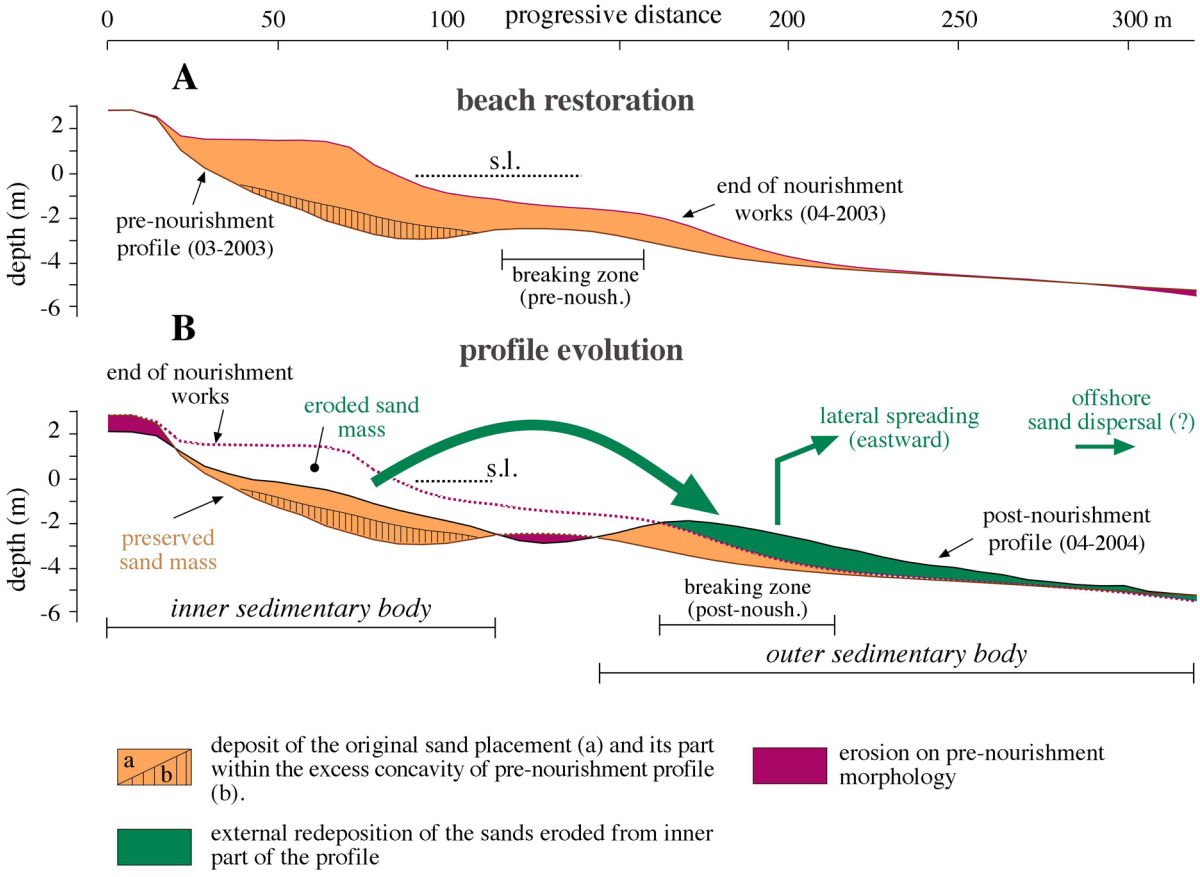

Fig. 12 - The artificial deposit immediately after nourishment (A) and a year later (B). Its evolution can be inferred from the superposition of the two profiles relating to these periods (B). Erosion and external sediment redeposition are the modalities by which the deposit has been reshaped. The inner sedimentary body corresponds to the preserved portion of the original sand placement, and the outer body to the redeposition of the unpreserved portion. The smaller green arrows refer to sediments spread laterally (eastward) and offshore from the outer sedimentary body. The excess concavity along the pre-nourishment profile was filled during beach replenishment operations.

topography related to the prevailing erosion conditions. This nourishment is distinguished by: (1) cross-shore sedimentary dynamics through which the nourished mass was reshaped; (2) beach widening far below expectations due to a concentrated deposition mainly at 3-4 m depth of the pre-fill bathymetry; (3) moderate loss of sediment, due to a lateral sand transport to the adjacent eastern coast; (3) inefficacy of the coastal structures (groins) in trapping the fill sands; (4) drastic resizing and swallowing of the breaking zone with possible feedback effects on nearshore hydraulic circulation. Each of these aspects was directly or indirectly conditioned by the borrow sand used, with a poor attitude to remain in equilibrium on the beach. In particular, the missed shoreline advance and consequent nourishment failure are due to the lack of coarse and medium sandy fractions in the borrow material compared to their abundance in the native beach sediments. Despite numerous inspections performed on different aspects, this study does not identify other significant causes or factors that may explain the intervention failure. In light of this failure and the unusual characteristics of the borrow sand (excessively sorted), eventual future extractions of sands from the large transgressive deposit off the coast of Capo D'Anzio should be carefully evaluated.

The grain size data used in this study are available as a supplementary file.

ACKNOWLEDGEMENTS - The Author is grateful to Regione Lazio for the access to the topographic and bathymetric data of Ladispoli Beach, and to E. Pranzini and S. Milli for their comments and suggestions that have significantly improved the manuscript.

REFERENCES

AA.VV., 1995. Atlante delle Spiagge Italiane. Dinamismo - Tendenza Evolutiva - Opere Umane. Fogli 149, 158. Progetto Finalizzato Conservazione del Suolo - Dinamica dei Litorali. CNR, MIUR, Selca, Florence, Italy.

Aragonés L., Pagán J.I., López I, Serra J.C., 2018. Depth of closure: new calculation method based on sediment data. International Journal of Sediment Research 33, 198-207.

Bellotti P., Davoli L., Sadori L., 2018. Landscape diachronic reconstruction in the Tiber delta during historical time: a holistic approach. Geografia Fisica e Dinamica Quaternaria 41, 3-21.

Bellotti P., De Luca G., 1979. Erosione del litorale del Lido di Roma: cause ed effetti. L'Universo 59, 1169-1182.

Bersani P., Bencivenga M., 2001. Le piene del Tevere a Roma dal V secolo a. C. all'anno 2000. Dipartimento Servizi Tecnici Nazionali, Servizio Idrografico e Mareografico Nazionale, Presidenza del Consiglio dei Ministri, Roma, 1-18.

Bird E., Lewis N., 2015. Beach renourishment. SpringerBriefs in Earth Sciences, Springer International Publishing, pp 137.

Birkemeier W.A., 1985. Field data on seaward limit of profile change. Journal of Waterway, Port, Coastal and Ocean Engineering 111, 598-602.

Bowen A.J., 1980. Simple model of nearshore sedimentation; beach profiles and longshore bars. In: Mac Cann S.B. (Ed.), The Coastline of Canada. Geological Survey of Canada, 1-11.

Caputo C., 1989. Il litorale laziale da Capo Linaro ad Anzio: caratteristiche fisiografiche e variazioni recenti della linea di riva. Rotary Club Viareggio - Versilia, Atti del Convegno "19° Forum: la fascia costiera tosco-ligure-laziale", Forte dei Marmi 26/27 settembre 1987, 31-38.

Caputo C., La Monica G.B., Lupia Palmieri E., Pugliese F., 1987. Phiyiographic characteristics and dynamics of the shore of Roma (Italy). In: Gardner (Ed.), Proceeding of the First International Conference on Geomorphology, Part I. John Wiley and Sons Ltd., 1185-1198.

Celia Magno M., Venti F., Bergamin L., Gaglianone G., Pierfranceschi G., Romano E., 2018. A comparison between laser granulometer and sedigraph in grain size analysis of marine sediments. Measurement 128, 231-236.

Cornaglia P., 1989. On Beaches. In: Fisher J.S., Dolan R. (Eds), Beach Processes and Coastal Hydrodynamics. Dowden Hutchingson and Ross, Stroudsburg, 11-26.

Cowell P.J., Kinsela M.A., 2018. Shoreface controls on barrier evolution and shoreline change. In: Moore L.J., Murray A.B. (Eds.), Barrier Dynamics and Response to Changing Climate. Springer International Publishing, 243-275.

Dean R.G., 2002. Beach Nourishment: Theory and Practice. World Scientific Publishing Co. New Jersey, pp. 399.

Dean R.G., 1991. Equilibrium beach profiles: characteristics and applications. Journal of Coastal Research 7, 53-84.

De Schipper M.A., De Vries S., Ruessink G., De Zeeuw R.C., Rutten J., Van Gelder-Maas C., Stive M.J.F., 2016. Initial spreading of a mega feeder nourishment: observations of the Sand Engine Pilot Project. Coastal Engineering 111, 23-38.

Elko N.A., Holman R.A., Gelfenbaum G., 2005. Quantifying the rapid evolution of a nourishment project with video imagery. Journal of Coastal Research 21, 633-645.

Everitt B.S., Landau S., Leese M., Stahl D., 2011. Cluster analysis. Wiley Series in Probability and Statistics, John Wiley & Sons Ltd., pp. 348.

Ferrante A., Franco L., Boer S., 1993. Modelling and monitoring of a perched beach at Lido di Ostia. In: Edge B. (Ed.), Proc. 23rd ICCE. Coastal Engineering 3, 3305-3318. ASCE, New York.

Folk R.L., Ward W.C., 1957. Brazos river bar: a study in the significance of grain size parameters. Journal of Sedimentary Petrology 27, 3-36.

Franco L., Di Risio M., Riccardi C., Scaloni P., Conti M., 2004. Monitoraggio del ripascimento protetto con barriera sommersa nella spiaggia di Ostia Centro. Studi Costieri 8, 3-16.

French P.W., 2005. Cross-shore variation of grain size on beaches. In: Schwartz M.L. (Ed.), Encyclopedia of Coastal Science. Springer Netherlands, 313-319.

Guillen J., Hoekstra P., 1996. The "equilibrium" distribution of grain size fractions and its implications for cross-shore sediment transport: a conceptual model. Marine Geology 135, 15-33.

Hallermeier R.J., 1978. Uses for a calculated limit depth to beach erosion. Proceedings 16th Internation Conference of Coastal

Engineering, HASCE, Hamburg, 1493-1512.

Hallermeier R.J., 1981. Seaward limit of significant by waves: an annual zonation for seasonal profiles. U.S. Army Corps of Engineers, Coastal Egineering Research Center CETA 81-2., pp. 24.

Hartman M., Kennedy A.B., 2016. Depth of closure over large regions using airborne bathymetric lidar. Marine Geology 379, 52-63.

Helland-Hansen W., Martinsen O.J., 1996. Shoreline trajectories and sequences: description of variable depositional-dip scenarios. Journal of Sedimentary Research 66, 670-688.

Hinton C., Nicholls R.J., 1998. Spatial and temporal behaviour of depth of closure along the Holland Coast. In: Edge B.L. (Ed.), 26th International Conference on Coastal Engineering ASCE, June 22-26 1998, Copenhagen, Denmark, 2913-2926.

Hobson R.D., 1977. Review of design elements for beach fill evaluation. U.S. Army Coastal Engineering Research Center, Technical Memorandum TM-77-6, pp. 51.

Huisman B.J.A., Walstra D.J., Radermacher M., De Schipper M.A., Ruessink BG., 2019. Observations and modelling of shoreface nourishment behaviour. Journal of Marine Science and Engineering 7, 59. doi: 10.3390/jmse7030059.

James W.R., 1974. Beach fill stability and borrow material texture. Proc. 14th International Conf. on Coastal Engineering, ASCE II, 1334-1344.

James W.R., 1975. Techniques in evaluating suitability of borrow material for beach nourishment. U.S. Army Coastal Engineering Research Center, Technical Memorandum 60, Vicksburg MS, pp. 82.

Kraus C., Larson M., Wise R., 1998. Depth of closure in beach fill design. In: Proceedings 12th National Conference on Beach Preservation Technology, Florida Shore and Beach Preservation Association 40, 271-286.

Krumbein W.C., James W.R., 1965. A lognormal size distribution model for estimating stability of beach fill material. U.S. Army Coastal Engineering Research Center, Technical Memorandum 16, pp. 17.

Mallandrino G.A., Novara A., Favara V., Viola F., 2014. Valutazione dell'efficacia degli interventi progettuali nella costa di Ladispoli. Meccanica dei Materiali e delle Strutture 4, 85-94.

Marinho B., Coelho C., Larson M., Hanson H., 2018. Short- and long-term responses of nourishments: Barra-Vagueira coastal stretch, Portugal. Journal of Coastal Conservation 22, 475-489.

Nicholls R.J., Larson M., Capobianco M., Birkemeier W.A., 1998. Depth of closure: improving understanding and prediction. In: In: Edge B.L. (Ed.), Proceedings of the Coastal Engineering Conference 3 ASCE, New York, 2888-2901.

Phillips M.R., Williams A., 2007. Depth of closure and shoreline indicators: empirical formulae for beach management. Journal of Coastal Research 23, 487-500.

Pilkey O.H, Young R.S., Riggs S.R., Smith A.W.S., Wu H., Pilkey W.D., 1993. The concept of shoreface profile of equilibrium: a critical review. Journal of Coastal Research 9, 255-278.

Pranzini E., 1999. Un indice di stabilità (Is) per la stima dell'idoneità dei materiali all'alimentazione artificiale delle spiagge. Studi Costieri 1, 75-83.

Pranzini E., Anfuso G., Munoz-Perez J.J., 2018. A probabilistic approach to borrow sediment selection in beach nourishment projects. Coastal Engineering 139, 32-35.

Psuty N.P., Ames K., Habeck A., Liu G., 2019. Sediment budget and geomorphological evolution of the estuarine dune-beach system on three nourished beaches, Delaware Bay, New Jersey. Geosciences 9, 16. doi: 10.3390/geosciences9010016.

Regione Lazio, 2003. Sintesi delle attività svolte: individuazione e caratterizzazione dei depositi sabbiosi presenti sulla piattaforma continentale della Regione Lazio e valutazione di un loro utilizzo ai fini del ripascimento dei litorali in erosione. Convenzione tra l'Università degli Studi di Roma "La Sapienza" Dipartimento di Scienze della Terra e la Regione Lazio, Fase Finale 2, 3, pp. 71.

Regione Lazio, 2013. Atlante della Dinamica Costiera Laziale (2005-2011), e-book, www.cmgizc.info/

Spodar A., Hequette A., Ruz M.H., Cartier A., Gregoire P., Sipka V., Forain N., 2018. Evolution of a beach nourishment project using dredged sand from navigation channel, Dunkirk, northern France. Journal of Coastal Conservation 22, 457-474.

Tarantola A., 2005. Inverse problem, theory and methods for model parameter estimation. Society for Industrial and Applied Mathematics, Philadelphia, pp. 342.

Tarragoni C., Bellotti P., Davoli L., Raffi R., Lupia Palmieri E., 2014. Assessment of coastal vulnerability to erosion: The case of Tiber River Delta (Tyrrhenian Sea, Central Italy). Italian Journal of Engineering Geology and Environment 2, 5-16.

Tortora P., 1992. Contributo dell'indagine sedimentologica al ripascimento dei litorali in erosione: ipotesi di ricostruzione della spiaggia di Marina di Tarquinia (Lazio settentrionale). Bollettino della Società Geologica Italiana 111, 315-333.

Tortora P., 2008. A new model for beach nourishment interventions: theory and applications. In: Pranzini E., Wezel L. (Eds.), Beach Erosion Monitoring. Nuova Grafica Fiorentina, Firenze, 207-228.

Tortora P., 2020. Failure of the nourishment intervention at Ladispoli Beach (Central Latium coast, Italy), Part 1: an insignificant episode during the last 70 years of coastal evolution. Journal of Mediterranean Earth Sciences 12, 33-53.

Tortora P., Cowell P.J., Adlam K., 2009. Transgressive coastal systems (2nd part): geometric principles of stratal preservation on gently sloping continental shelves. Journal of Mediterranean Earth Sciences 1, 15-32.

USACE, 2008. Beach Fill Design. In: Coastal Engineering Manual, US Army Corps of Engineers, EM 1110-2-1100 (Part V, chapter 4), pp. 109.

Valiente N.G., Masselink G., Scott T., Conley D., McCarroll R.J., 2019. Role of waves and tides on depth of closure and potential for headland bypassing. Marine Geology 407, 60-75.

Verhagen H.J., 1996. Analysis of beach nourishment schemes. Journal of Coastal Research 12, 179-185.

Wentworth C.K., 1922. A scale of grade and class terms for clastic sediments. Journal of Geology 30, 377-392.